

Master Degree course in Communications Engineering

Master Degree Thesis

# Performance Evaluation of NOMA and OFDMA in LEO Satellite Constellations

Supervisors

Prof. Roberto Garello

Candidate
Selim UCAR

## Contents

1	Inti	roduction	2		
	1.1	Motivation	2		
	1.2	Scope of the Study	3		
	1.3	Thesis Organization	3		
2	LEO Satellite Communications				
	2.1	Overview of Satellite Communication Systems	4		
	2.2	Characteristics of LEO Satellite Constellations	5		
	2.3	Challenges in LEO Satellite Communication	5		
	2.4	Multiple Access Techniques in Satellite Networks	6		
3	Non-Orthogonal Multiple Access (NOMA) in Satellite Communications				
	3.1	Principles of NOMA	8		
	3.2	Performance Analysis and Simulative Approach to NOMA in Satellite			
		Communication	10		
4	Orthogonal Frequency-Division Multiple Access (OFDMA) in Satellite				
	Cor	nmunications	14		
	4.1	Principles of OFDMA	14		
	4.2	Performance Analysis and Simulative Approach to OFDMA in Satellite			
		Communication	17		
5	System Model and Software Simulation				
	5.1	Methodology and Model Description	21		
	5.2	Simulation Parameters and Implementation	21		
	5.3	Performance Metrics and Results	23		
6	Cor	nclusion and Future Work	42		
Ribliography					

## Acknowledgements

This page is intentionally left blank.

#### Abstract

Low Earth Orbit (LEO) satellite constellations are emerging as a cornerstone of nextgeneration communication infrastructures, and their significance for Internet of Things (IoT) ecosystems continues to grow steadily. LEO satellites operate at considerably lower orbital altitudes, thereby mitigating signal propagation delays and significantly reducing communication latency. The adoption of advanced multiple access techniques is indispensable, as they have to manage scarce spectral resources while supporting the exponential growth in the number of connected devices. Such techniques are required not only to enhance spectral efficiency and maximize achievable throughput but also to ensure robust and reliable connectivity in highly dynamic and interference-prone LEO environments. Consequently, the selection and design of multiple access schemes represent a critical factor in determining the overall performance, scalability, and quality of service of LEO-based communication systems. This thesis investigates the performance of Non-Orthogonal Multiple Access (NOMA) and Orthogonal Frequency Division Multiple Access (OFDMA) in LEO satellite communication networks. A heuristic-based software simulation environment is developed to model a satellite constellation system in Walker Delta form and evaluate the comparative performance of these two multiple access techniques. The study primarily focuses on Signal-to-Interference-plus-Noise Ratio (SINR), system capacity, data rates, spectral efficiency, and varying satellite constellation network conditions. By conducting comprehensive simulations, this research aims to provide insights into the suitability of NOMA and OFDMA for LEO constellations for IoT applications and high-speed internet service in Ka-band. The findings contribute to the ongoing efforts to enhance access strategies for next-generation satellite networks.

## Chapter 1

## Introduction

## 1.1 Motivation

The rapid expansion of Low Earth Orbit (LEO) satellite constellations is revolutionizing global communication networks, particularly in enabling the Internet of Things (IoT) on a large scale. The ability of LEO satellites to provide low-latency and widespread connectivity makes them an essential component in future wireless communication systems. However, as the number of IoT devices continues to grow exponentially, efficient multiple access techniques become crucial to managing the limited spectral resources effectively while ensuring reliable data transmission [1].

In terrestrial networks, Non-Orthogonal Multiple Access (NOMA) and Orthogonal Frequency Division Multiplexing (OFDM) have been extensively studied for their ability to enhance spectral efficiency and support massive connectivity [2]. However, their application in LEO-based satellite communications remains an open research challenge due to the dynamic nature of satellite links and variations in network topology. Evaluating the performance of these techniques in a LEO satellite environment is essential to determine their feasibility for IoT applications and next-generation satellite communication networks and constellation formations.

This thesis aims to bridge this gap by developing a Python-based software simulation environment to model a LEO satellite constellation and analyze the comparative performance of NOMA and OFDMA. The key performance metrics include system capacity, spectral efficiency, and latency, considering different satellite network conditions. By visualizing and comparing the simulation results, this study provides valuable insights into the advantages and limitations of these multiple access techniques in a satellite-based IoT ecosystem.

The findings of this research contribute to the ongoing efforts in optimizing multiple access strategies for future LEO satellite networks, supporting the seamless integration of IoT devices and enhancing global connectivity.

## 1.2 Scope of the Study

This study focuses on evaluating the performance of two prominent multiple access techniques, NOMA and OFDMA, in the context of LEO satellite constellations. The research aims to analyze their effectiveness in handling the growing demand for high spectral efficiency, low latency, and massive connectivity, which are critical for emerging IoT applications and next-generation satellite communications.

The scope is limited to downlink scenarios and considers key performance indicators such as system capacity, spectral efficiency, and latency. A Python-based software simulation environment is developed to model LEO satellite behavior, including realistic channel characteristics and constellation parameters. The study does not include hardware implementation or terrestrial network integration but remains focused on the simulative comparison and theoretical analysis of NOMA and OFDMA under different satellite network conditions.

By restricting the analysis to these parameters and scenarios, the research aims to deliver a clear understanding of how each technique performs in isolation within a satellite communication framework and to support future decision-making processes regarding multiple access strategies in LEO constellations.

## 1.3 Thesis Organization

This thesis is structured into two main phases, each contributing to a comprehensive evaluation of NOMA and OFDMA techniques within LEO satellite constellations.

The first phase is dedicated to the theoretical and mathematical modeling of both NOMA and OFDMA schemes in the context of LEO satellite communication. This includes the derivation of mathematical models, performance indicators, and comparative analysis between the two methods. Emphasis is placed on evaluating the theoretically expected outcomes in terms of spectral efficiency, system capacity, and latency, while considering the unique characteristics and challenges of satellite environments such as number of satellites in the shell and altitude.

In the second phase, a simulation environment is developed using a software-based approach to model a single-shell LEO satellite constellation. Within this model, the performance of NOMA and OFDMA is examined under practical conditions. The simulation takes into account key system parameters such as satellite altitude, the number of satellites per shell, and channel characteristics. Performance metrics include latency, spectral efficiency, system capacity, and the influence of constellation design on communication efficiency.

## Chapter 2

## LEO Satellite Communications

## 2.1 Overview of Satellite Communication Systems

Satellite communication systems facilitate crucial long-distance connectivity by utilizing orbiting satellites as relay stations in space to transmit signals beyond the line of sight [3]. A system of this nature generally comprises a space segment, which includes the satellite or constellation operating in orbit, and a ground segment, consisting of Earth-based control stations and user terminals.

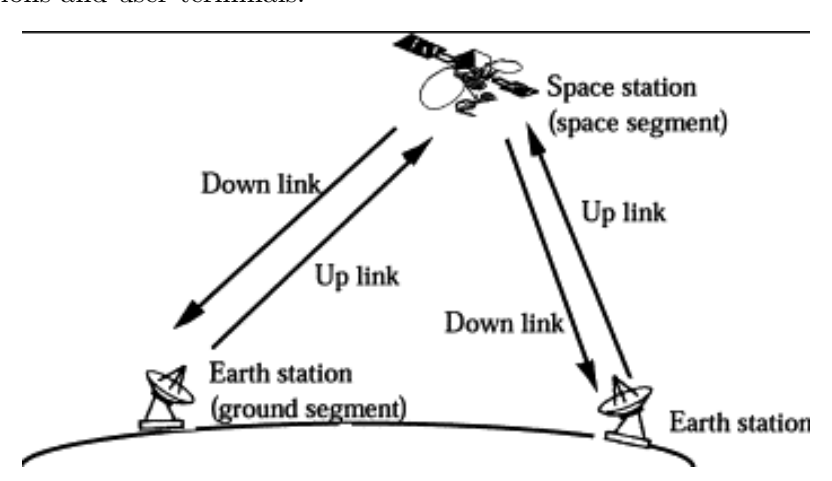


Figure 2.1: Overview Diagram of Satellite Communications

Communication is facilitated through an uplink, whereby a transmitting Earth station sends signals to the satellite, followed by a transponder onboard the satellite that receives and amplifies the signal, and a downlink that retransmits the signal to a receiving station. This system architecture enables diverse applications such as global voice and data telecommunications, television broadcasting, broadband Internet access, and connectivity for maritime, aeronautical, and remote areas where terrestrial networks are not feasible. Satellites can be categorized into four principal types based on their orbital characteristics [4]:

• Low Earth Orbit (LEO): These satellites operate at altitudes ranging from 200 to

2,000 kilometers above Earth's surface.

- Medium Earth Orbit (MEO): Positioned primarily between 8,000 and 20,000 kilometers above Earth's surface, MEO satellites are commonly utilized for navigation systems like GPS and communication networks.
- Geostationary Earth Orbit (GEO): Also referred to as the Clarke Orbit, these satellites maintain a fixed position at an altitude of 35,786 kilometers above the equator.
- Highly Elliptical Orbit (HEO): Characterized by a highly eccentric trajectory, these satellites can reach altitudes of up to 40,000 kilometers at apogee (the farthest point from Earth).

## 2.2 Characteristics of LEO Satellite Constellations

A Low Earth Orbit (LEO), as indicated by its nomenclature, refers to an orbital path that is comparatively proximate to the terrestrial surface of the Earth. LEO satellites are deployed at altitudes below 2,000 kilometers. This upper boundary is largely determined by the presence of the Van Allen radiation belts, whose intense radiation environment creates harsh conditions for spacecraft operating at higher altitudes. The minimum altitude at which a satellite can operate is dictated by the influence of the Earth's atmosphere. Typically, satellites are not deployed at altitudes lower than 180 kilometers for this specific rationale — while this is relatively low in the context of other orbits, it remains significantly elevated above the Earth's surface. In this context, communications satellites positioned in Low Earth Orbit (LEO) frequently operate as components of a constellation, which constitutes a network of multiple identical or analogous satellites collaborating to deliver uninterrupted coverage in a 'net' configuration encircling the Earth. This principle similarly extends to constellations utilized for observation or navigation purposes [5].

Satellites dedicated to specific applications, such as Earth observation, rely on efficient mechanisms for transmitting the data they collect. Typically, this data is transmitted via a downlink that is configured to match the rate of data collection. However, in cases where real-time transmission is not feasible, Low Earth Orbit (LEO) satellites are equipped with onboard memory systems to store the collected data during their orbit. Once the satellite comes within range of a receiving Earth station, the stored information is downloaded, ensuring the continuity of data acquisition and delivery [6].

## 2.3 Challenges in LEO Satellite Communication

Low Earth Orbit (LEO) satellite networks, while offering the advantage of reduced propagation delays, present unique technical challenges due to their low altitude and high orbital velocity. A key issue arises from the significant Doppler shift introduced by the rapid relative motion of satellites, which can reach 950 Hz frequency shift [7]. At GHz operating frequencies, this results in frequency deviations of several tens of kilohertz

which is substantially higher than those observed in terrestrial communication system and demands the implementation of sophisticated Doppler compensation techniques.

Additionally, since LEO satellites have short orbital periods, they are visible to a given ground terminal for only a few minutes. Continuous connectivity requires frequent handovers between satellites, adding further complexity to the network design [8].

## 2.4 Multiple Access Techniques in Satellite Networks

In satellite communications, multiple access refers to the ability of several users to simultaneously utilize a shared resource, such as a satellite's transponder. The transponder functions as the communication medium, receiving signals from terrestrial terminals via the uplink and retransmitting them back to Earth through the downlink to the designated users. These users are spread across different geographical locations, and various techniques are employed to enable their concurrent access to the satellite's transponder.

Multiple Access Techniques play a crucial role in satellite networks. Commonly used, legacy techniques are Frequency Division Multiple Access (FDMA), Time Division Multiple Access (TDMA), Code Division Multiple Access (CDMA) and Space Domain Multiple Access (SDMA) [9]:

- Frequency Division Multiple Access (FDMA): Allocates distinct frequency bands to different users, ensuring that each user has a dedicated frequency channel for the duration of their communication session. In the context of Frequency Division Multiple Access (FDMA), multiple Earth stations can access the entire available bandwidth of the satellite transponder by utilizing distinct carrier frequencies, thereby preventing interference between the signals from different users.
- Time Division Multiple Access (TDMA): Allocates distinct time slots to individual users within a recurring frame structure. Each user transmits during their assigned time slot, enabling multiple users to use the same frequency channel without causing interference. In Time Division Multiple Access (TDMA), various Earth stations within the satellite's coverage area share the transponder by utilizing a single carrier in a time-division manner. This should not be confused with Time Division Multiplexing (TDM), which is a technique employed at a specific Earth station to transmit multiple digitized baseband signals simultaneously over a shared communication channel, with each signal being separated in time.
- Code Division Multiple Access (CDMA): Allows multiple users to transmit at the same time over the same frequency band by assigning a unique code to each user. The receiver uses these codes to separate the signals from different users. In CDMA, multiple Earth stations utilize the full bandwidth of the transponder simultaneously. Each transmitter spreads its signal across the entire bandwidth, which is significantly wider than the bandwidth needed for the signal. One method of achieving this is by multiplying the information signal with a pseudorandom bit sequence.
- Space Domain Multiple Access (SDMA): Space Division Multiple Access (SDMA) is an advanced technique in satellite communications that uses spatial separation

to allow multiple users to share the same frequency channel at the same time. Through the use of smart antennas or phased arrays, SDMA directs concentrated beams towards specific users, effectively creating distinct spatial channels within the same frequency band [10]. By applying the SDMA technique on a single satellite platform, multiple beams with different polarizations can cover the same area of the Earth's surface, enabling frequency re—use. In a typical satellite link, SDMA is often combined with other multiple access techniques like FDMA, TDMA, and CDMA.

The most commonly used multiple access techniques have been briefly discussed. In the scope of this thesis, however, the focus will be specifically on NOMA and OFDMA techniques, and a comparative and simulation based implementation of these methods will be carried out. Chapter 3 will provide a detailed discussion of the NOMA technique, both mathematically and practically. Chapter 4 is dedicated to the OFDMA technique, following the same structure. In this section, we will also present an overview of the application of NOMA and OFDMA techniques in satellite networks.

In context of satellite communications, NOMA is regarded as a crucial technology for supporting terrestrial 5G applications, particularly those involving massive machine-type communications (mMTC) as can be seen in Eutelsat fleet [11]. NOMA is a multiple access method that enables several users to utilize the same time—frequency resources by layering their signals in the power domain. In contrast to orthogonal approaches like OFDMA or TDMA, NOMA uses power-domain multiplexing and relies on Successive Interference Cancellation (SIC) at the receiver to distinguish and separate the users' signals [12].

On the other hand, Orthogonal Frequency Division Multiplexing (OFDM) is a digital modulation technique that partitions a high—speed data stream into several lower rate subcarriers, with each subcarrier carrying a segment of the data. This approach improves spectral efficiency and offers resilience against channel impairments, including multipath fading. In the context of satellite networks, OFDMA is employed to enhance the reliability and efficiency of data transmission, effectively mitigating issues such as Doppler shifts and high mobility.

To obtain a higher spectral efficiency in wireless communications has led to the proposal of hybrid NOMA-OFDM solutions [13]. However, there is currently no solid or widely adopted study specifically demonstrating the combined use of these techniques in LEO satellite constellations.

## Chapter 3

# Non-Orthogonal Multiple Access (NOMA) in Satellite Communications

## 3.1 Principles of NOMA

Non-orthogonal multiple access (NOMA) has emerged as a leading candidate among advanced radio access techniques envisioned for next-generation wireless communication systems. Unlike the widely adopted Orthogonal Frequency Division Multiple Access (OFDMA), which is the standard orthogonal multiple access (OMA) scheme in current networks, NOMA enables multiple users to share the same time, frequency, and spatial resources simultaneously. NOMA transmits users' signals by superimposing them based on their power levels. On the receiver side, the signals are separated using the Successive Interference Cancellation (SIC) technique. SIC in NOMA is a receiver-side method that processes overlapping user signals step by step. After successfully decoding one user's signal, it subtracts it from the combined received signal, allowing the receiver to decode the next user. This process enables multiple users to efficiently share the same frequency and time resources. In this way, the same resources can be shared by multiple users, resulting in enhanced spectral efficiency. Furthermore, NOMA is capable of supporting ultra-reliable low-latency communications and massive connectivity, which are critical requirements for applications such as the Internet of Things (IoT) and machine-type communications. These advantages position NOMA as a compelling solution for meeting the performance demands of future wireless networks. A schematic belonging to the NOMA method can be seen in Figure 3.1 below:

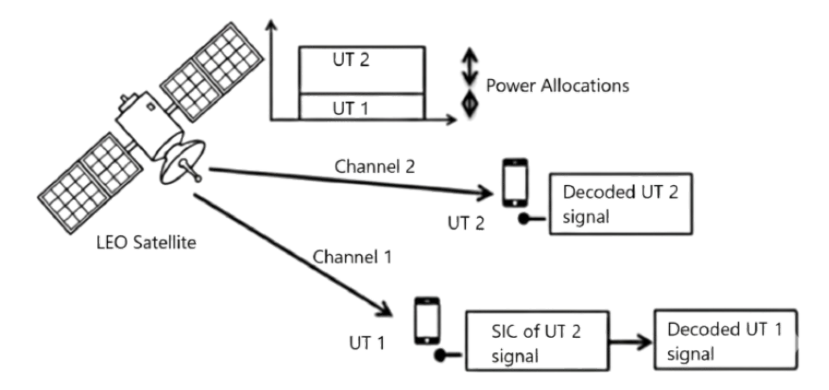


Figure 3.1: NOMA System Schematic

In light of this information, we can model the signal of a LEO satellite as follows. Consider a scenario in which the downlink communicates with N users and M satellites in the LEO constellation shell. After establishing the signal model, the fundamental SAT-COM parameters should also be considered. These can be listed as follows: Propagation loss, geometric antenna pattern, and channel statistical properties.

#### Channel Gain Between User and Satellite

In a LEO satellite constellation with M satellites and N users, the complex channel gain between the m-th satellite and the k-th user is modeled as:

$$h_{m,k} = \sqrt{\frac{G_{s,m}(\theta_{m,k}) \cdot G_{u,k}}{L_{m,k}}}$$

$$(3.1)$$

where:

- $G_{s,m}(\theta_{m,k})$ : antenna gain of satellite m toward user k, depending on beam angle  $\theta_{m,k}$ ,
- $G_{u,k}$ : antenna gain of user k's terminal,
- $L_{m,k}$ : free-space path loss between satellite m and user k, given by

$$L_{m,k} = \left(\frac{4\pi d_{m,k} f_c}{c}\right)^2 \tag{3.2}$$

•  $d_{m,k}$ : distance between satellite m and user k,

## Superposition Signal Model by Satellite m

Assuming satellite m serves a subset of users  $\mathcal{U}_m \subseteq \{1, \ldots, N\}$ , the NOMA downlink signal transmitted by satellite m is:

$$x_m(t) = \sum_{k \in \mathcal{U}_m} \sqrt{\alpha_{m,k} P_m} \, x_k(t) \tag{3.3}$$

where:

- $\alpha_{m,k}$ : power allocation factor for user k from satellite m (with  $\sum_{k\in\mathcal{U}_m}\alpha_{m,k}=1$ ),
- $P_m$ : total transmit power of satellite m,
- $x_k(t)$ : baseband signal intended for user k.

### Signal to Interference Plus Noise Ratio for LEO Constellation NOMA

Assume satellite  $m \in \{1, 2, ..., M\}$  serves a subset of users  $\mathcal{U}_m \subseteq \{1, 2, ..., N\}$  via downlink NOMA. For user  $k \in \mathcal{U}_m$ , let the users be ordered according to their channel gains as seen by satellite m, such that:

$$|h_{m,1}|^2 \le |h_{m,2}|^2 \le \dots \le |h_{m,|\mathcal{U}_m|}|^2$$
 (3.4)

Then, the SINR of user k served by satellite m, after applying SIC for users with weaker channels is:

$$SINR_{m,k} = \frac{\alpha_{m,k} |h_{m,k}|^2 P_m}{\sum_{r=k+1}^{|\mathcal{U}_m|} \alpha_{m,r} |h_{m,k}|^2 P_m + \sigma^2}$$
(3.5)

where:

- $\alpha_{m,k}$ : power allocated by satellite m to user k (with  $\sum_{k \in \mathcal{U}_m} \alpha_{m,k} = 1$ ),
- $P_m$ : total transmit power of satellite m,
- $h_{m,k}$ : channel gain from satellite m to user k,
- $\sigma^2$ : noise power (if you keep  $N_0$ , use  $\sigma^2 = N_0 B$ ).

# 3.2 Performance Analysis and Simulative Approach to NOMA in Satellite Communication

In the context of LEO satellite constellations, the deployment of NOMA across multiple equivalent satellites introduces a set of unique performance evaluation criteria. Consider a scenario where a constellation of M equivalent LEO satellites collectively serves N ground users through downlink NOMA transmission. In such a system, several key parameters influence overall performance and must be modeled accordingly.

In this study, during performance calculations, frequency values will be taken in the range of Ka— band, which are frequently used in LEO satellite constellations. In the European region, the Ka-band range is defined between 27,5 GHz and 31 GHz [14].

We will consider a downlink NOMA system with M satellites serving a total of N users under a Rayleigh fading model. Each satellite can serve multiple users on the same time/frequency resource using power-domain multiplexing. Successive Interference Cancellation (SIC) is assumed to exist at the receivers, allowing higher-channel-quality

users to cancel interference from lower-channel-quality users. Key parameters are defined as follows:

- M: Number of satellites (downlink transmitters in the system).
- N: Total number of users served by all satellites (indexed as needed per satellite).
- $N_m$ : Number of users served by satellite m (so  $\sum_{m=1}^{M} N_m = N$ ).
- $\alpha_{m,k}$ : Power allocation coefficient for user k on satellite m (power-domain NOMA), with  $\sum_{k=1}^{N_m} \alpha_{m,k} = 1$ . (If you keep  $P_{m,k}$  elsewhere, use  $P_{m,k} \equiv \alpha_{m,k} P_m$ .)
- $P_m$ : Total transmit power of satellite m.
- $h_{m,k}$ : Channel coefficient (complex fading gain) from satellite m to its k-th user. Let  $g_{m,k} = |h_{m,k}|^2$  denote the channel power gain.
- $\sigma^2$ : Noise power (variance of additive white Gaussian noise) at each user's receiver.

Within each satellite's user group we sort users by their channel conditions. Assume  $g_{m,1} \leq g_{m,2} \leq \cdots \leq g_{m,N_m}$ , meaning user 1 has the weakest channel on satellite m (and will be allocated the highest power), while user  $N_m$  has the strongest channel (allocated the lowest power). In the power-based NOMA scheme, users with stronger channels perform SIC to remove interference from signals intended for users with weaker channels (who have higher transmit power), thereby improving their own reception. The following formulas give the requested performance metrics in mathematical form.

#### 3.2.1 SINR for Each User

For a given satellite m, consider its k-th user (with channel gain  $g_{m,k}$  and allocated power  $P_{m,k}$ ). Under ideal SIC, this user will decode and cancel interference from all users j < k (those with weaker channels but higher allocated power) before decoding its own signal. It will treat signals of users j > k (stronger channel users with lower power) as noise since those are not decoded prior to its own signal. Thus, the Signal-to-Interference-plus-Noise Ratio (SINR) for user k on satellite m can be expressed as:

SINR<sub>m,k</sub> = 
$$\frac{P_{m,k} g_{m,k}}{\sum_{j=k+1}^{N_m} P_{m,j} g_{m,k} + \sigma^2}$$
, (3.6)

where the summation in the denominator represents the remaining intra-satellite interference (ISI) from users  $j=k+1,k+2,\ldots,N_m$  (those with better channel conditions who are not canceled by user k's SIC process). In this formula,  $P_{m,k}g_{m,k}$  is the received signal power for user k's own signal, and  $\sum_{j=k+1}^{N_m} P_{m,j}g_{m,k}$  is the total interference power at this user from all other signals on the same satellite that have not been removed via SIC. Note that user k=1 (the weakest user) has no prior users to cancel, so its SINR includes interference from all other  $j=2,\ldots,N_m$  users. Conversely, user  $k=N_m$  (the strongest user) can cancel interference from all  $j< N_m$ , so its SINR is limited only by noise (and possibly inter-satellite interference if present, which is neglected here assuming orthogonal resource allocation between satellites).

#### 3.2.2 Total Transmitted Power

The total transmitted power in the system is the sum of the transmit powers allocated to all users across all M satellites. If each satellite m has a total power budget  $P_{m,\text{tot}} = \sum_{k=1}^{N_m} P_{m,k}$ , then the system-wide total transmit power is given by:

$$P_{\text{total}} = \sum_{m=1}^{M} \sum_{k=1}^{N_m} P_{m,k} = \sum_{m=1}^{M} P_{m,\text{tot}}.$$
 (3.7)

So, we accumulated the power of every user's superposed signal. In a power-domain NOMA scheme,  $P_{m,k}$  may often be written as a fraction of  $P_{m,\text{tot}}$  (e.g.  $P_{m,k} = \alpha_{m,k}, P_{m,\text{tot}}$  with  $\sum_k \alpha_{m,k} = 1$  for each satellite), but the formula above remains general. It captures the fact that all user signals on all satellites contribute to the total transmitted power in the network.

## 3.2.3 Sum Rate of the NOMA System

The sum rate is the aggregate data rate achieved by all users in the system. Assuming each user's channel capacity is achieved with Gaussian signaling, the rate for user k on satellite m can be expressed by the Shannon formula  $R_{m,k} = B, \log_2 (1 + \text{SINR}_{m,k})$ , where B is the bandwidth (in Hz) allocated to the NOMA transmission (or one unit bandwidth if normalized). Under the assumption that all N users share the same time-frequency resource (per satellite) and can achieve these individual rates simultaneously via SIC, the total sum rate of all users in the system is:

$$R_{\text{sum}} = \sum_{m=1}^{M} \sum_{k=1}^{N_m} B \log_2 \left( 1 + \text{SINR}_{m,k} \right)$$
 (3.8)

- $\bullet$  M is the number of satellites,
- $N_m$  is the number of users served by satellite m,
- SINR<sub>m,k</sub> is the signal-to-interference-plus-noise ratio for the k-th user served by satellite m.

In this expression,  $SINR_{m,k}$  is substituted from the formula in metric (1) for each user. The sum rate  $R_{sum}$  represents the combined throughput of the N users. It inherently accounts for NOMA's power-domain multiplexing and SIC. The summation adds up all these contributions. This sum rate would typically be compared against an equivalent orthogonal multiple access (OMA) scenario to illustrate NOMA's spectral efficiency gains, given appropriate power allocation and successful interference cancellation. Sum rate defines the system capacity and throughput as well. Theoretical total system capacity can be proved as:

$$C_{\text{sat}} = \sum_{u} B \log_2 \left( 1 + \text{SINR}_u \right), \tag{3.9}$$

 $C_{sat}$  stands for the satellites capacity and  $B_{sat}$  is the bandwidth per satellite (100MHz default in the simulation). Deriving from the system SINR and sum rate  $R_{sum}$ , data

rate per user can be calculated. In order to do this, system should be considered under user-per-satellite (UPS) condition. Aim is to detect and provide hight data rates to the user clusters in the satellite coverage area.

$$SINR_{m,k}^{(\varepsilon)} = \frac{P_{m,k} g_{m,k}}{\varepsilon \sum_{j=1}^{k-1} P_{m,j} g_{m,k} + \sum_{j=k+1}^{N_m} P_{m,j} g_{m,k} + I_{m,k} + \sigma^2},$$
 (3.10)

$$r_{m,k} = B \log_2(1 + SINR_{m,k}^{(\varepsilon)})$$
 [Mbit/s] (3.11)

## 3.2.4 Spectral Efficiency

Spectral efficiency (SE) quantifies how efficiently the available bandwidth is utilized in transmitting data. It is defined as the total achievable sum rate of the system normalized by the bandwidth:

$$\eta = \frac{R_{\text{sum}}}{B} \tag{3.12}$$

where:

- $\eta$  is the spectral efficiency in bits per second per Hertz (bits/s/Hz),
- $R_{\text{sum}}$  is the total sum rate achieved by all users in the system (in bits/s),
- B is the system bandwidth in Hertz (Hz).

Spectral efficiency increases with better SINR, efficient power allocation, and effective interference cancellation (such as ideal SIC in NOMA). Therefore, it serves as a key metric for evaluating the capacity performance of multiple access schemes in LEO satellite networks.

## Chapter 4

## Orthogonal Frequency-Division Multiple Access (OFDMA) in Satellite Communications

## 4.1 Principles of OFDMA

Orthogonal Frequency Division Multiplexing (OFDMA) is a multicarrier transmission technique designed for high data rate communication systems. It works by distributing high-speed data across numerous low-rate subcarriers. These subcarriers are mutually orthogonal, and their frequency separation is achieved through the application of the Fast Fourier Transform (FFT) [15].

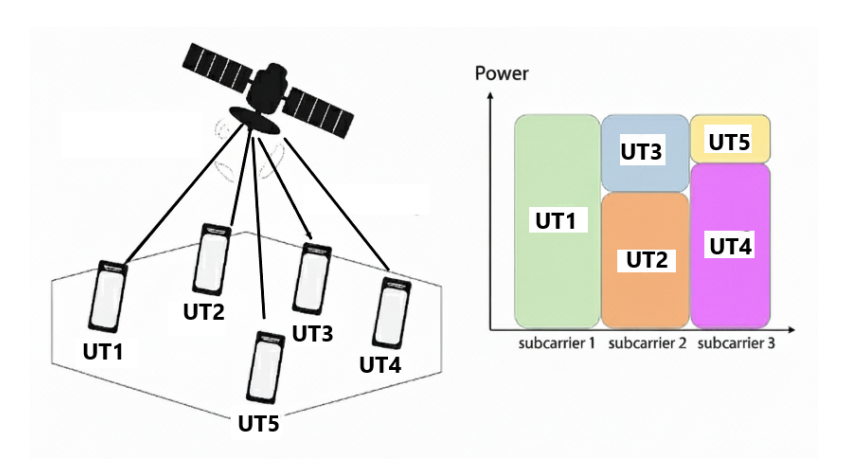


Figure 4.1: OFDMA System Schematic

Considering OFDMA in satellite communications, each user is assigned a distinct group of subcarriers, enabling concurrent downlink transmissions without interference assuming ideal conditions. Unlike traditional single-user OFDM, which dedicates all subcarriers to one user in a given time slot, OFDMA supports flexible subcarrier allocation

among multiple users. This adaptability makes OFDMA particularly effective for LEO satellite systems, where user link conditions and satellite coverage vary frequently. A fundamental concept in OFDMA, carried over from OFDM, is the orthogonality of its subcarriers. Each subcarrier is a sinusoidal signal, and they are spaced in frequency so that they remain orthogonal over the symbol period T; in other words, their cross-correlation equals zero during this time interval. Expected advantages of OFDMA application in LEO constellations follow:

- Enhanced Bandwidth Utilization: OFDMA enables concurrent access to the same frequency band by multiple users, resulting in more efficient use of available spectrum—particularly beneficial in densely populated networks.
- Lower Transmission Delay: By allocating subcarriers according to user demands, OFDMA minimizes data transmission delays. This is essential for latency-sensitive applications such as real-time video streaming and interactive gaming.
- Improved Performance in High-Traffic Scenarios: In environments with heavy user density—like stadiums or airports—OFDMA alleviates network congestion by supporting simultaneous communication for many devices.
- Adaptive Resource Allocation: OFDMA supports dynamic distribution of subcarriers, ensuring that high-bandwidth tasks (e.g., video conferencing) receive more resources, while low-bandwidth tasks (e.g., IoT sensors) are assigned fewer.
- Greater Energy Efficiency: Through optimal transmission scheduling, OFDMA minimizes the active time of user devices. This reduces power consumption, which is especially advantageous for battery-dependent equipment such as smartphones and IoT nodes.

Signals transmitted between the user and the satellite can follow multiple propagation paths, with each path introducing distinct phase shifts and time delays. Reflections from the Earth's surface or atmospheric layers may add smaller, secondary delays. While modeling the channel, the overall delay is represented as a combination of the dominant geometric delay and the minor delays introduced by multipath components.

Delay spread describes the time-domain dispersion resulting from these multipath effects. In OFDM systems, this is typically addressed using a cyclic prefix (CP). The length of the CP is designed to exceed the maximum expected delay spread, which helps to eliminate intersymbol interference (ISI). This ensures that each subcarrier retains orthogonality and avoids interference with adjacent symbols.

#### 4.1.1 OFDMA Signal Model with Rayleigh Fading and Doppler Shift

Each user k = 1, 2, ..., N transmits an OFDMA signal as follows:

$$x_k[n] = \sum_{l=0}^{L-1} \sum_{q \in \mathcal{N}_{k,l}} s_{k,q}[l] e^{j\frac{2\pi q}{N} (n-lN_s)} g[n-lN_s]$$
 (4.1)

where:

- $s_k[l]$ : The l-th IFFT output symbol for user k,
- $f_{k,l}$ : Subcarrier frequency assigned to user k,
- g[n]: Pulse shaping window function (e.g., RRC),
- $N_s$ : OFDM symbol duration (including cyclic prefix),
- L: Number of OFDM symbols.

#### **OFDMA Channel Model**

The time-varying multipath Rayleigh fading channel between user k and satellite m is modeled as:

$$h_{k,m}(t,\tau) = \sum_{p=1}^{P} \alpha_{k,m,p}(t)\delta(\tau - \tau_p)$$
(4.2)

where:

- $\alpha_{k,m,p}(t)$ : Complex Gaussian path gain,  $\sim \mathcal{CN}(0,\sigma_p^2)$ ,
- $\tau_p$ : Delay of the p-th path,
- P: Number of multipaths.

Doppler shift for user k to satellite m is:

$$f_{D,k,m} = \frac{v_{k,m} f_c}{c} \cos(\theta_{k,m}) \tag{4.3}$$

where:

- $v_{k,m}$ : Relative velocity between user k and satellite m,
- $f_c$ : Carrier frequency,
- c: Speed of light,
- $\theta_{k,m}$ : Angle of arrival.

The received signal at satellite m is the superposition of all user signals:

$$y_m[n] = \sum_{k=1}^K \sum_{p=1}^P \alpha_{k,m,p}[n] \ x_k[n-d_p] \ e^{j2\pi f_{D,k,m} \ nT_s} + w_m[n]$$
 (4.4)

where:

- $T_s$ : Sampling interval,
- $w_m[n] \sim \mathcal{CN}(0, \sigma_w^2)$ : Additive white Gaussian noise.

Assuming downlink transmission from M satellites:

$$y_k[n] = \sum_{m=1}^{M} \sum_{p=1}^{P} \alpha_{k,m,p}[n] x_m[n - d_p] e^{j2\pi f_{D,k,m} nT_s} + w_k[n]$$
 (4.5)

# 4.2 Performance Analysis and Simulative Approach to OFDMA in Satellite Communication

#### 4.2.1 SINR Calculation for OFDMA Users

The SINR for user k served by satellite m on subcarrier n can be expressed as [16]:

$$SINR_{m,k,n} = \frac{P_{m,k,n} |h_{m,k,n}|^2}{\sum_{j \neq m} P_{j,k,n} |h_{j,k,n}|^2 + \sigma^2}$$
(4.6)

$$h_{m,k,n}[l] = \sum_{p=1}^{P} \alpha_{k,m,p}[l] e^{-j 2\pi n \Delta f \tau_p}$$
(4.7)

where:

- $P_{m,k,n}$  is the power allocated to user k on subcarrier n by satellite m,
- $h_{m,k,n}$  is the channel gain between satellite m and user k on subcarrier n,
- The denominator includes inter-satellite interference (from all  $j \neq m$ ) and the noise power  $\sigma^2 = N_0 \Delta f_n$ .

## 4.2.2 Resource Allocation and Power Control

OFDMA performance heavily depends on efficient resource allocation strategies [17]. The optimization problem for maximizing system capacity can be formulated as:

maximize: 
$$\sum_{m=1}^{M} \sum_{k=1}^{N_m} \sum_{n=1}^{N} x_{m,k,n} \Delta f_n \log_2(1 + \text{SINR}_{m,k,n})$$
subject to: 
$$\sum_{k=1}^{N_m} \sum_{n=1}^{N} P_{m,k,n} \leq P_{\text{max},m}, \quad \forall m \quad \text{(Power constraints)}$$

$$\sum_{k=1}^{N_m} x_{m,k,n} \leq 1, \quad \forall m,n \quad \text{(Subcarrier allocation)}$$

$$0 \leq P_{m,k,n} \leq x_{m,k,n} P_{\text{max},m}, \quad \forall m,k,n \quad \text{(Coupling)}$$
QoS requirements per user.

where:

- $x_{m,k,n} \in \{0,1\}$ : binary allocation variable;  $x_{m,k,n} = 1$  if subcarrier n is assigned to user k on satellite m.
- $P_{m,k,n} \ge 0$ : transmit power allocated by satellite m to user k on subcarrier n (coupled via  $0 \le P_{m,k,n} \le x_{m,k,n} P_{\max,m}$ ).
- $P_{\max,m}$ : total power budget of satellite m (constraint  $\sum_{k=1}^{N_m} \sum_{n=1}^{N} P_{m,k,n} \leq P_{\max,m}$ ).

- $\Delta f_n$ : bandwidth of subcarrier n (Hz); typically  $\sum_{n=1}^N \Delta f_n = B$  under the chosen reuse pattern.
- N: total number of subcarriers;  $N_m$ : number of users served by satellite m.

#### 4.2.3 Inter Carrier Interference

In LEO satellite communication systems, the high relative velocities between the satellites and ground terminals introduce significant Doppler shifts, which can severely disrupt the orthogonality of subcarriers in OFDM-based waveforms. This orthogonality is essential for ensuring that each subcarrier can transmit data independently without interference from others. When Doppler-induced frequency shifts become comparable to or exceed the subcarrier spacing, the spectral overlap between adjacent subcarriers increases, leading to inter-carrier interference (ICI). ICI manifests as unwanted energy leakage from neighboring subcarriers, degrading signal quality and making accurate demodulation more challenging. The power of ICI experienced by a given subcarrier can be quantified by summing the interference contributions from all other subcarriers, and is directly influenced by factors such as Doppler spread, subcarrier spacing, and the receiver's ability to compensate for frequency shifts. Without effective Doppler compensation techniques, the presence of ICI can significantly reduce the performance and spectral efficiency of the communication system.

The average ICI power for different sequences can be approximated as [18]:

$$\overline{\sigma_{\text{ICI}}^m} = \sum_{\substack{i_{\text{ICI}} \neq s_{\text{ICI}} \\ i_{\text{ICI}} = 0}}^{N-1} \left| P\left(\frac{i_{\text{ICI}} - s_{\text{ICI}}}{T} + \Delta f\right) \right|^2$$
(4.9)

- N: Total number of subcarriers.
- T: OFDM symbol duration.
- $\Delta f$ : Frequency offset (due to Doppler shift).
- $s_{ICI}$ : Desired symbol location.
- $i_{ICI}$ : Index of all subcarriers, used to analyze the power of other subcarriers.

## 4.2.4 Co-channel Interference (CCI)

Co-channel interference (CCI) in OFDMA systems refers to the disruption that arises when multiple transmitters such as satellites or beams operate on the same frequency resources (e.g., subcarriers), resulting in overlapping signals at the receiver. In mathematical expressions of OFDMA, this interference is typically included in the SINR formula as an additional interference power component added to the denominator [19].

$$CCI_{k,n} = \sum_{s' \neq s} P_{s',k,n}^{RX}$$

$$(4.10)$$

- $P_{s',k,n}^{\text{RX}}$ : received co-channel power at user k from interfering satellite/beam s' on subcarrier n.
- The sum runs over all satellites/beams s' except the serving one s for user k on subcarrier n.

In LEO satellite communications, the impact of CCI is strongly influenced by the number of satellites. And this effect will be examined practically in the performance evaluation chapter.

## 4.2.5 Sum Rate of the OFDMA System

The theoretical system capacity and the sum rate in the OFDMA method, much like in NOMA, is based on the Shannon principle. Fundamentally, it is defined as a cumulative sum that is directly proportional to the signal-to-interference-plus-noise ratio (SINR).

$$R_{\text{sum}} = \sum_{m=1}^{M} \sum_{k=1}^{N_m} \sum_{n=1}^{N} x_{m,k,n} \, \Delta f_n \, \log_2 \left( 1 + \text{SINR}_{m,k,n} \right). \tag{4.11}$$

- M is the number of satellites,
- $N_m$  is the number of users served by satellite m,
- SINR<sub>m,k,n</sub> is the signal-to-interference-plus-noise ratio for the k-th user on subcarrier n from satellite m.

The entire bandwidth in an OFDMA system is partitioned into series of narrow frequency bands, each serving as an orthogonal subcarrier. Each of these subcarriers functions as a distinct communication channel, and thanks to their orthogonality, they avoid mutual interference under ideal conditions. This allows for the capacity of each subcarrier to be determined separately using the Shannon theorem. The achievable data rate for a single subcarrier is a function of its dedicated bandwidth and its Signal-to-Noise Ratio (SNR) or Signal-to-Interference-plus-Noise Ratio (SINR) value, as expressed below:

$$C_{\text{sys}} = \sum_{m=1}^{M} \sum_{k=1}^{N_m} \sum_{n=1}^{N} x_{m,k,n} \, \Delta f_n \, \log_2(1 + \text{SINR}_{m,k,n})$$
 (4.12)

 $\Delta f$  represents the frequency spacing and is obtained by dividing the total bandwidth by the number of subcarriers. Subsequently, to determine the total capacity, this calculation is aggregated over the total number of subcarriers and across the entire constellation, and capacity per satellite will be accumulated through the changing satellite count. During the simulation phase, it will be assumed that all subcarriers have uniform and almost equal SINR values.

Following the discussion in Chapter 4, where effects such as ICI and CCI were addressed, the system SINR formula has been updated. The final SINR formula, which will be used in capacity and data rate calculations, is as follows:

$$SINR_{m,k,n} = \frac{P_{m,k,n} |h_{m,k,n}|^2}{\sigma^2 + CCI_{k,n} + \sigma_{ICI}^{(m)}(\Delta f)}$$
(4.13)

Combining the knowledge so far, one can obtain the average per-user data rate in OFDMA system:

$$r_u^{\text{OFDMA}} = \Delta f_n \log_2 \left( 1 + \frac{P_{m,k,n} |h_{m,k,n}|^2}{\underbrace{\sigma^2}_{\text{noise}} + \underbrace{\text{CCI}_{k,n}}_{\text{co-channel}} + \underbrace{\sigma_{\text{ICI}}^{(m)}(\Delta f)}_{\text{ICI}} \right)$$
(4.14)

- m: Serving satellite (or beam) index for user k on subcarrier n.
- $P_{m,k,n}$ : Transmit power allocated to user k on subcarrier n by serving satellite m.
- $h_{m,k,n}$ : Channel coefficient from satellite m to user k on subcarrier n;  $|h_{m,k,n}|^2$  is the channel power gain (path loss + fading, etc.).
- $\sigma^2$ : Noise power on subcarrier n (W).
- s: Serving satellite/beam index on that subcarrier; s': interfering satellites/beams.
- $P_{s',k,n}^{\text{RX}}$ : Received co-channel power at user k from interferer s' on subcarrier n.
- $CCI_{k,n}$ : Co-channel interference term (represented by the underbrace in the denominator).
- $\sigma^{(m)}_{\text{ICI}}(\Delta f)$ : Inter-carrier interference power for the serving link, modeled as a function of Doppler-induced frequency offset  $\Delta f$
- $\Delta f$  vs.  $\Delta f_n$ :  $\Delta f$  (inside  $\sigma_{\rm ICI}^{(m)}$ ) is the Doppler offset (Hz);  $\Delta f_n$  is the subcarrier bandwidth (Hz).

The mathematical model to be implemented in the simulation and performance evaluation phase is depicted as follows. In a scenario where the user density within the coverage area is a key constellation parameter, the capacity and data rate formulas will be aggregated across the user-per-satellite (UPS) value, which serves as the simulation input.

#### 4.2.6 Spectral Efficiency in OFDMA

The spectral efficiency for OFDMA in LEO systems should account for [20]:

$$\eta_{\text{OFDMA}} = \frac{1}{B_{tot}} \sum_{m=1}^{M} \sum_{k=1}^{N_m} \sum_{n=1}^{N} x_{m,k,n} \, \Delta f_n \, \log_2(1 + \text{SINR}_{m,k,n}), \qquad B_{tot} = \sum_{n=1}^{N} \Delta f_n$$
(4.15)

- $B_{tot}$ : Total system bandwidth across subcarriers (Hz).
- M: The total number of satellites in the system.
- $N_m$ : The total number of users within the coverage area of satellite m.
- N: The total number of subcarriers in the system.

where the efficiency depends on the effectiveness of resource allocation algorithms and interference management. Unlike NOMA's power-domain multiplexing, OFDMA achieves multiplexing through orthogonal subcarrier allocation.

## Chapter 5

# System Model and Software Simulation

## 5.1 Methodology and Model Description

In this chapter, a simulation environment was developed using Python 3.10 to create a virtual replica of the system and to examine the performance of the aforementioned multiple access methods within a LEO constellation. The coding was carried out based on object-oriented programming. Entities such as system parameters and orbital elements were implemented using the Poliastro library and map projection is done using Cartopy library. Subsequently, antenna parameters were defined as a class, and each user was processed within a loop to run the simulation. The NumPy library was used for numerical and mathematical operations, while Matplotlib was employed to plot the resulting visual and graphical outputs. Throughout this chapter, the theoretical mathematical analyses covered in the previous four chapters will be simulated using this methodology, and the resulting outcomes will be examined.

## 5.2 Simulation Parameters and Implementation

In the simulation, communication system operating in the Ka-band at 28 GHz with an overall system bandwidth of 100 MHz. The constellation comprises an array of M satellites over Europe region sharing the same shell, each concurrently serving N users. These two values are kept independent variables in each simulation. Since antenna design is not in the scope of this study, for simplicity, all users and satellites are considered as ideal parabolic antennas with a 50 dBi gain and 1m of diameter. Spot beam architecture is realized in antenna model. The wireless channels between satellites and users are modeled as independent Rayleigh fading channels, with small-scale fading effects represented by exponentially distributed channel power gains due to multipath propagation.

In the downlink scenario considered, each satellite transmits data to its associated users. Interference between satellites ("inter-satellite interference") is considered based on an assumption of orthogonal frequency allocation. The analysis further neglects intersymbol interference to focus exclusively on multiple-access effects.

The total downlink transmit power per satellite remains the same for both schemes but differs in its allocation among users. For SINR, spectral efficiency, system capacity and data rate evaluation, a Monte Carlo (20 iterations) simulation is performed: random Rayleigh fading realizations are generated per user, signal-to-interference-plus-noise ratio (SINR) values and corresponding per-user spectral efficiencies and rates are computed. The M number of satellites in the constellation have been simulated using Walker Delta orbital configuration, similar [21]. Within the scope of this study, only users located in the European region and the satellites serving them have been considered. A global view and the regional view of the constellation configuration are illustrated in the figures below.

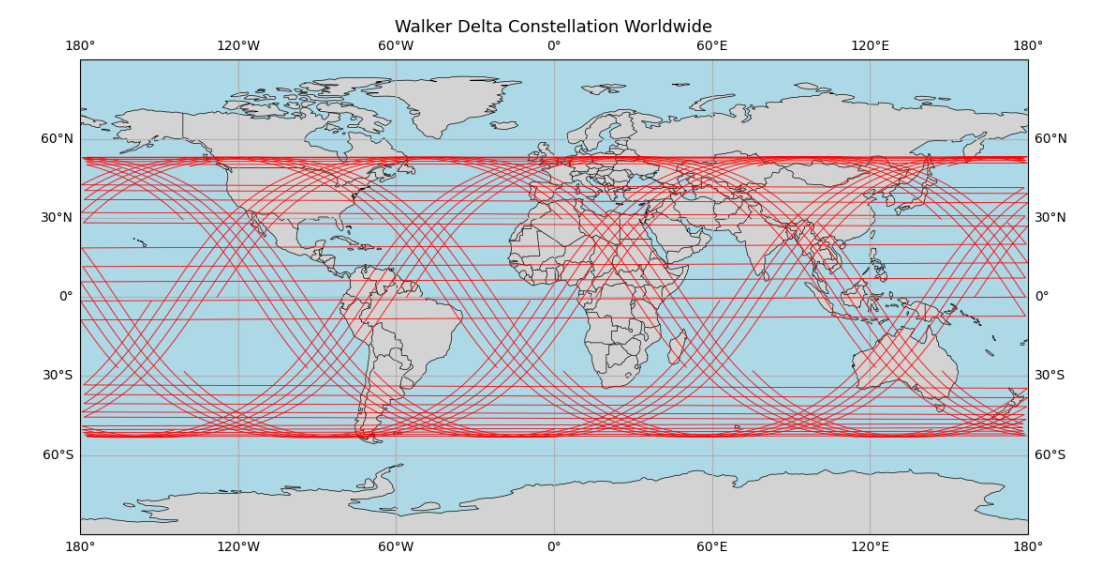


Figure 5.1: Walker Delta Constellation – Global View

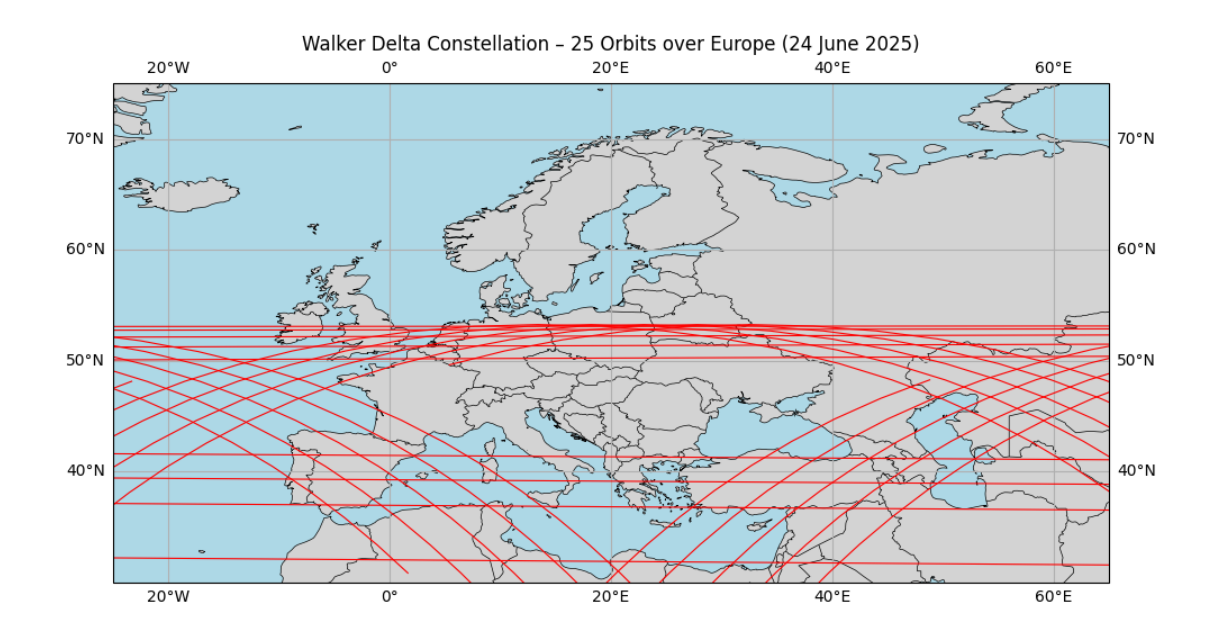


Figure 5.2: Walker Delta Constellation – Europe Region

However, this configuration of the constellation corresponds to a reference point at the initial timestamp, the initial value. Therefore, over time, the orbits will progress westward, eventually covering the entire intended coverage area. The performance metrics of the multiple access methods will be evaluated based on a reference timestamp at which M satellites are actively serving the European region.

## 5.3 Performance Metrics and Results

## 5.3.1 SINR Analysis of NOMA Downlink

The signal-to-interference-plus-noise ratio (SINR) is a key metric for evaluating the performance of Non-Orthogonal Multiple Access (NOMA) in satellite communication systems. NOMA allows multiple users to share the same resources (time/frequency/space), usually through superposition coding and successive interference cancellation (SIC). In this performance evaluation simulation, a simplified approach is followed and it is assumed that SIC is applied for all receivers successfully, without considering the actual waveforms.

In order to calculate and analysis the SINR values of the system, Equation 3.6 is converted to a Python function. A previous study in this field suggests that the functioning of NOMA in LEO satellite networks and its advantage was observed only when the target SINR remained below a specific threshold [22].

Inter-satellite interference and successive interference cancellation (SIC) are two critical factors in SINR analysis, directly influencing the computation. SIC is a key component of the NOMA method and is addressed in Chapter 3 of this thesis. In the simulation,

SIC is modeled as a residual factor ranging between 0 and 1. A value of 0 represents a perfect and dominant SIC, meaning that the user with a power allocation advantage can completely eliminate interference from other users. The extreme case where the factor equals 0 represents perfect SIC, in which inter-user interference is entirely eliminated. On the other hand, a factor value of 1 corresponds to a scenario where SIC is not applied at all, leading to the worst-case SINR performance.

An increase in the number of satellites in the constellation—i.e., satellite terminals—can lead to performance improvement due to the reduced number of users per satellite. This expectation is based on the assumption that channel interference decreases, hence a decrease in the intra-satellite interference. However, as the number of satellites in the constellation increases, so does the number of interfering satellites, thereby intensifying inter-satellite interference. Therefore, the number of satellites with overlapping coverage areas and the number of served user terminals should be maintained at an optimal level.

To ensure optimal service quality of the constellation, the number of users within the coverage area and their power allocation must be carefully optimized. In the simulation conducted for this purpose, a fixed power allocation scheme compatible with SIC principles was applied. In this scenario, the number of satellites in the constellation was increased, satellites falling within the inter-satellite interference range were considered, and under these conditions, a heatmap was generated based on the number of user terminals served by satellites providing overlapping coverage.

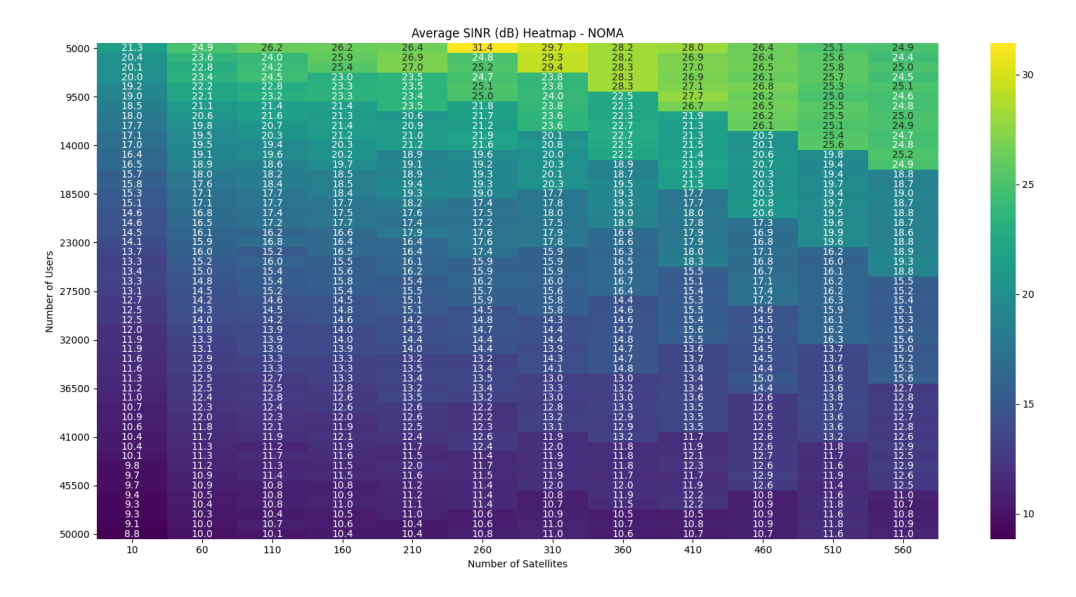


Figure 5.3: Average SINR (dB) Heatmap, NOMA, SIC = 0.1

Figure 5.3. displays the average per-user SINR (dB) versus constellation size, 10-560 satellites and load 5,000-50,000 users under highly effective SIC. At light load, around 5,000 users, SINR extends from  $\sim 21$ ,dB down to a global maximum of 31,4 dB around 260 satellites and then remains high but gradually decreases (e.g., 29,7 dB at 310, 28,2

dB at 360, 28 dB at 410, and 24,9,dB at 560). With increasing numbers of users, SINR smoothens down: at 9,500 users the typical values are 19–26,dB (with  $\approx 25.0$ ,dB around 260 satellites); locally peaked near 21,6–22,5 dB around 260–360 satellites. Even at the maximum 50,000-user load, the SINR remains around 9–11,dB (e.g., 8,8,dB at 10 satellites and around 11,6,dB at 510 satellites). Overall, SINR improves markedly with constellation densification up to roughly 260–310 satellites for a given load, whilst heavier loading erodes these gains and drives the system towards a flatter  $\approx 10$ –12 dB regime.

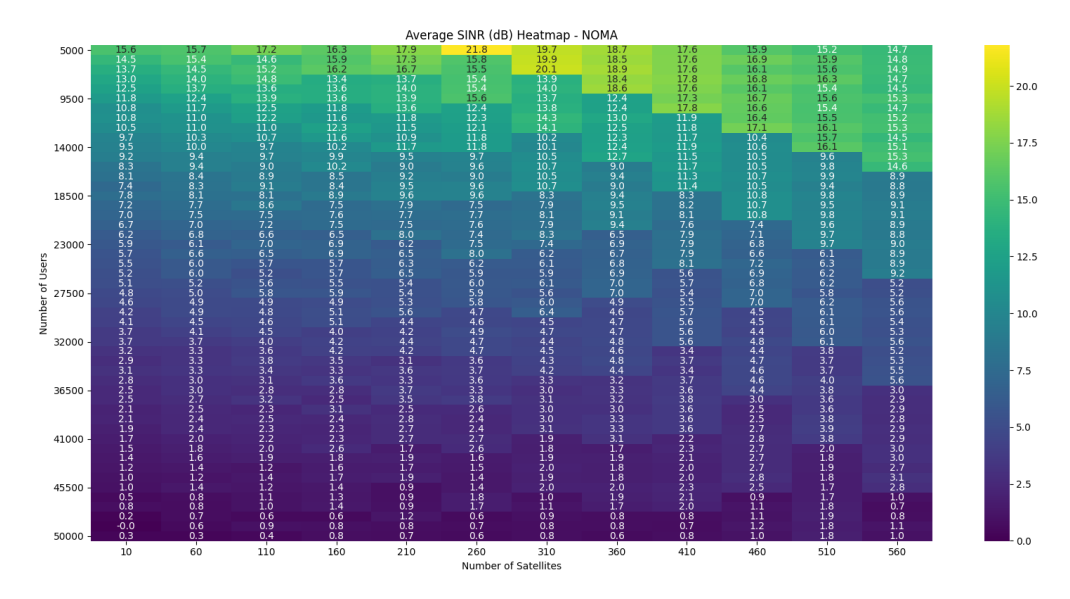


Figure 5.4: Average SINR (dB) Heatmap, NOMA, SIC = 0.5

The heatmap reports the average per-user SINR (dB) as a function of constellation size, 10--560 satellites and offered load 5,000–50,000 users. At light load (5,000 users), SINR spans roughly 15–22dB and peaks around 21,8 dB at  $\sim$  260 satellites; a second local maximum of about 20,1 dB appears at 9,500 users and  $\sim$  310 satellites. As the number of users increases, SINR degrades steadily: at 18,500 users typical values are 8–11 dB (e.g. 10,8 dB at  $\sim$  460 satellites), around 23,000–32,000 users it falls to 3–7dB, and at 50 000 users it is  $\leq$  1–2dB across most constellation sizes (e.g. 0.3dB at 10 satellites and  $\sim$  1,0 dB at 560). Along the satellite axis, SINR generally improves with densification up to  $\sim$  260–310 satellites and then rolls off mildly beyond  $\sim$  400, reflecting increasing interference coupling. Practically, maintaining  $\geq$  10 dB average SINR requires keeping the load below  $\sim$  14,000–18,500 users for mid-to-large constellations, whereas heavier loads drive the system into the < 5 dB regime where NOMA performance becomes interference-limited.

Two different SIC values were included in the comparison. A low SIC value represents a nearly perfect SIC implementation. In this context, it can be observed that the average SINR values increase in the scenario with SIC = 0.1 but not significantly. However, increasing the number of satellites in the constellation does not always lead to higher SINR values. It is observed that in both cases, the configuration with approximately  $\approx 260$  satellites in the constellation represents an optimal point in terms of performance

and reliability. As SIC quality degrades, the overall SINR level decreases; however, the optimal range remains relatively stable.

## 5.3.2 SINR Analysis of OFDMA Downlink

The SINR analysis of the constellation continues with the downlink calculations for the OFDMA method. At this stage, two critical factors influence SINR performance: intercarrier interference (ICI) and co-channel interference (CCI). These concepts have been discussed in detail in the theoretical framework presented in Chapter 4. From a performance evaluation perspective, both types of interference are inversely proportional to the SINR value.

Hence, ICI directly results from Doppler shift and negatively impacts the orthogonality of OFDMA subcarriers, whereas CCI arises when different satellites employ the same subcarrier, leading to interference [23]. As evident, this section's SINR performance analysis for OFDMA will focus on two variable parameters: Doppler shift will play a more prominent role, and, similar to the NOMA scenario, an increasing number of satellites in the constellation will cause greater channel interference, thereby degrading SINR. Therefore, an optimization between the number of satellites and the number of users served within the same coverage area will be pursued.

The simulation's Inter-Carrier Interference (ICI) and Co-Channel Interference (CCI) indices are grounded in established physical models from the literature. The ICI is modeled as a function of Doppler shift, which results from the high orbital speeds of LEO satellites. Each user's Doppler frequency is calculated dynamically using the formulation [24]. This model captures the loss of subcarrier orthogonality due to satellite-user relative motion, with ICI power scaling proportionally to the square of the ratio between Doppler shift and subcarrier spacing. Meanwhile, the CCI model accounts for interference stemming from increased satellite coverage overlap and spectral congestion due to higher user densities. As the number of users sharing a subcarrier rises, the CCI impact intensifies. These interference models are consistent with recent studies [25] and are scaled using normalized constants to align with typical ICI and CCI levels in Kaband LEO satellite networks, accurately representing the main sources of degradation in OFDMA-based systems realistically. Figures regarding the results can be seen below.

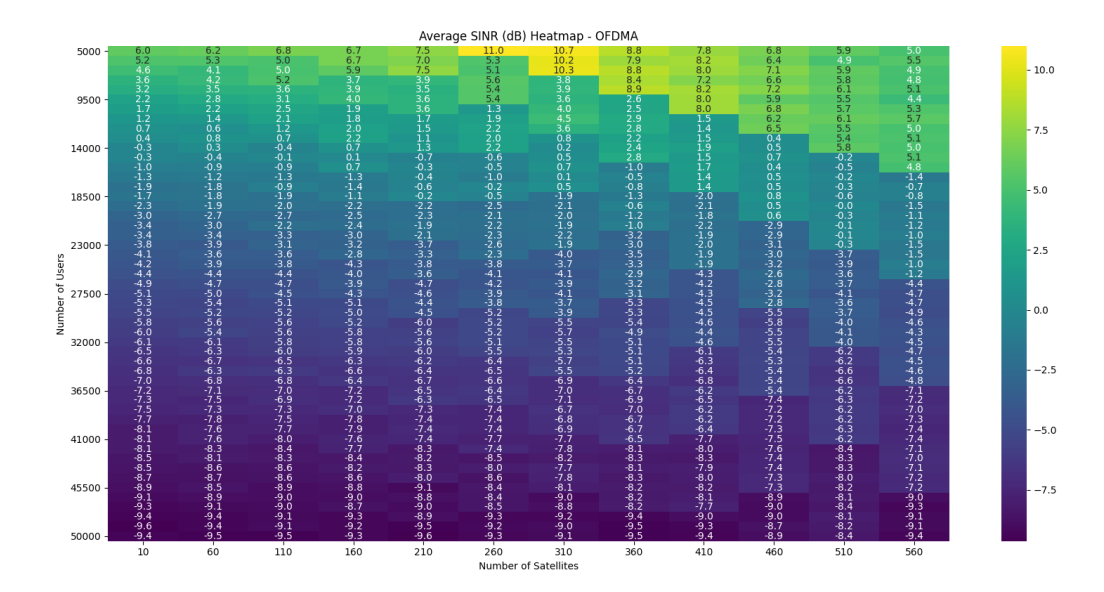


Figure 5.5: Average SINR (dB) Heatmap, OFDMA,  $N_{sc}=64$ 

Figure 5.5. reports the average per-user SINR (dB) versus constellation size (10–560 satellites) and offered load (5,000–50,000 users). At light load (5,000 users), SINR ranges from 6,0 to a global peak of 11,0 dB near 260 satellites (then 10,7 dB at 310, 8.8 dB at 360, and 5,0 dB at 560). At 9,500 users, typical values lie between 2 and 8 dB, reaching  $\sim$  8.0 dB around 410 satellites. With increasing UT count, SINR declines rapidly: by 14,000 users it hovers around 0–5 dB, and beyond 23,000 users the map is predominantly negative (e.g., -3.8 to -0.1 dB). Heavier UT loads push the system further into the noise dominant regime, with  $\approx$  –4 to –6 dB around 32,000 users and  $\approx$  –9 to –8,9 dB at 50,000 users across most constellation sizes. For a fixed load, densifying the constellation improves SINR up to roughly 260–310 satellites, after which gains saturate and slightly roll off towards 560 satellites.

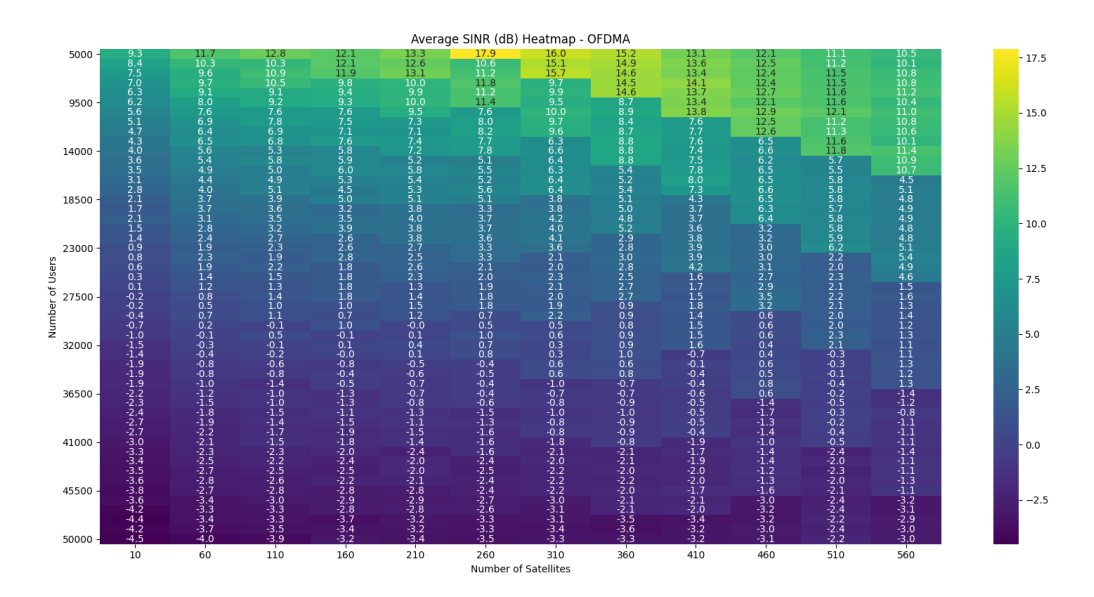


Figure 5.6: Average SINR (dB) Heatmap, OFDMA,  $N_{sc} = 256$ 

Then Figure 5.6. shows the average per-user SINR (dB) versus constellation size (10–560 satellites) this time with  $N_{sc}=256$ , and load (5,000–50,000 users). At lower UT counts such as 5,000 users, SINR spans 9,3–17,9 dB, attaining a global maximum of 17,9 dB at  $\sim 260$  satellites and then tapering to 16,0 dB (310), 15,2 dB (360), 13,1 dB (410), 12,1 dB (460), 11,1 dB (510) and 10,5 dB (560). At 9,500 users, values remain clearly positive ( $\sim 6$ –14dB), with a ridge across 210–410 satellites (e.g., 11.4 dB at 260 and 13,6 dB at 360). Beyond 36,500 users the system becomes interference-limited for most constellation sizes, and at 50,000 users the SINR is predominantly negative (approximately -4,5 to -3,0 dB, e.g., -4,5 dB at 10 satellites and -3,0 dB at 560). Overall, increasing  $N_{\rm sc}$  to 256 substantially elevates the SINR ridge and sustains positive SINR to higher loads.

The downlink SINR calculations for the scenario in which the constellation operates using the OFDMA multiple access technique are illustrated in the heatmaps presented in Figures 5.5 and 5.6. In the simulation, the arrays for the number of users and the number of satellites in the constellation were kept consistent with those defined in Chapter 5.1. The Inter-Carrier Interference (ICI), which is influenced by Doppler shift and thus affects SINR, is modeled dynamically based on the altitude of the satellite communicating with the user (i.e., lower altitudes lead to higher Doppler effects). For the Co-Channel Interference (CCI), the primary contributing factor is the number of users per subcarrier. While an uncontrolled increase in the number of satellites enhances spatial coverage by increasing the number of transmitters, it also introduces additional interference. In the simulation, users are uniformly distributed across subcarriers so the congested traffic such as 4 subcarriers for 1000 users is avoided. As a result, the expected trend is a decrease in CCI with a lower user-to-subcarrier ratio, but a rise in CCI with an increasing number of satellites. In this context, system-level optimization is pursued.

Based on the simulation outcomes, it can be inferred that the optimal configuration

for this system is  $\approx 260$  satellites serving  $\approx 5,000$  user terminals. Additionally, increasing the number of subcarriers delays system saturation, thereby contributing to an overall improvement in capacity.

With the SINR tests in consideration of NOMA and SINR methods, for the downlink Ka-band scenario (  $f \approx 28$  GHz) having a 100 MHz overall bandwidth, simulations vary the satellites' quantity ( M ) and the user quantity ( N ) in a European coverage region employing a Walker-Delta shell at a constant reference time. Satellites and user terminals employ ideal parabolic antennas ( $f \approx 50$  dBi gain, 1m diameter) and a spot-beam architecture, and user–satellite connections are modelled by individual Rayleigh-faded connections. Inter and Intra Satellite Interferences are considered in the calculations. Inter-Symbol Interference (ISI) and atmospheric attenuations are neglected.

## 5.3.3 Spectral Efficiency

Low Earth Orbit (LEO) satellite networks require highly efficient spectrum utilization to meet the demands of higher data rates in Ka-band and large-scale user connectivity. Non-Orthogonal Multiple Access (NOMA) has gained attention as a promising technique to improve spectral efficiency by enabling multiple users to simultaneously access the same time and frequency resources. This contrasts with Orthogonal Frequency Division Multiple Access (OFDMA), where users are allocated distinct frequency bands. In the context of LEO satellite constellations, where optimal spectrum usage is vital, NOMA offers a significant capacity advantage over traditional Orthogonal Multiple Access (OMA) methods. Additionally, conventional OMA techniques like OFDMA encounter limitations in LEO environments due to factors such as high Doppler shifts and long propagation delays, further highlighting the need to explore NOMA-based solutions for future satellite communication systems. Therefore, in this performance evaluation simulation, the expected outcome is that the NOMA method will provide higher spectral efficiency under the same conditions. However, the goal of this chapter is not limited to a comparison between these multiple access methods. It will also examine optimal user pairing strategy in the satellite constellation to achieve high spectral efficiency.

## 5.3.4 Spectral Efficiency Analysis of NOMA Downlink

In LEO satellite communication systems utilizing Non-Orthogonal Multiple Access (NOMA), spectral efficiency serves as a key performance indicator that reflects the system's ability to make optimal use of its spectrum resources. Unlike traditional orthogonal multiple access methods, NOMA enables multiple users to simultaneously access the same time-frequency blocks by leveraging power domain multiplexing and employing successive interference cancellation (SIC) to separate overlapping signals. While calculating spectral efficiency, the average SINR values computed in the previous chapter were retrieved from the simulation memory to ensure system consistency. Since the power allocation must be compatible with SIC, the Gain Ratio Power Allocation (GRPA) method was adopted. This means that SIC was neither neglected nor assumed to be perfect during the spectral efficiency evaluation. Instead, a fixed SIC value of 0.1 was used throughout the simulation. Naturally, due to its dependence on SINR, a degradation in SIC performance is

expected to lead to a decrease in spectral efficiency.

A direct correlation between the sum rate (Eq. 3.12) and spectral efficiency was observed. An ideal parabolic antenna was assumed to guide the power budget, and this value was treated as a variable simulation input. Subsequently, based on Equation 3.6, the sum rate was calculated over the constellation's satellite and ground terminal arrays. In this simulation, modulation formats were not treated as variables. For the downlink, 16QAM modulation was kept fixed, as it is practical and consistent with the obtained SINR values. The signal and channel models described in Chapter 3 were implemented accordingly. After 20 iterative Monte Carlo runs, the results obtained from the spectral efficiency calculation in the NOMA system are presented in the figure below.

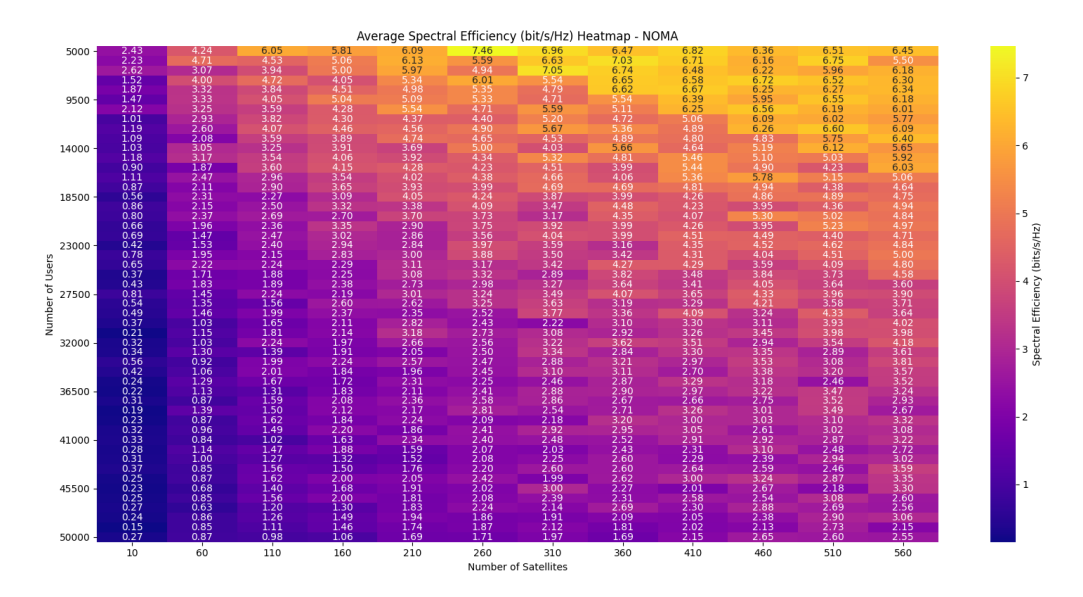


Figure 5.7: Spectral Efficiency Heatmap for NOMA System

Figure 5.7 shows the average downlink NOMA spectral efficiency as a function of constellation size and UT count. The efficiency grows as the constellation gets denser and reaches approximately 7,4 bit/s/Hz in a broad region around 260–310 satellites under a light load in which approximately two satellites have the same power budget on average; beyond this point the advantage fades. With a larger number of satellites the efficiency drops because more satellites enjoy the same power budget and more residual intra-cluster interference accumulates, and a visible decline appears once the load gets above about three UTs per satellite. The results were computed by the use of GRPA power allocation and a fixed SIC residue of 0,1 in the 28 GHz, 100 MHz Ka-band configuration and support the earlier analysis in terms of SINR showing  $\approx 260$  satellites serving  $\approx 5,000$  UTs.

Upon examining the heatmap obtained from the simulation results, it can be observed that the NOMA multiple access method provides reasonable spectral efficiency for LEO satellite constellations with a high number of satellites operating within the same orbital shell. The most critical factor is the ability of the satellites to uniformly distribute the users within their coverage areas. Scenarios where each satellite serves, on average, two

user terminals tend to achieve higher spectral efficiency. However, once the number of user terminals per satellite exceeds three, a decline in efficiency is observed. The obtained results are applicable to IoT applications in the Ka-band, as they closely reflect realistic values when considering large constellations like Starlink [26].

## 5.3.5 Spectral Efficiency Analysis of OFDMA Downlink

In the constellation simulation, the spectral efficiency calculation for the OFDMA multiple access method is based on Equation 4.15. As proven by this formula, the primary factors affecting the system's spectral efficiency are the number of subcarriers, the number of satellites and users, and the bandwidth. Since a uniform and hypothetical system is considered, the bandwidth is kept constant in the spectral efficiency calculations—just as in the SINR evaluations—because this parameter is appropriately selected for the Kaband, which is independent of the constellation design. As discussed in the previous subchapter, the number of subcarriers significantly influences the system's SINR, and thus the spectral efficiency, based on the user-to-subcarrier ratio. To avoid redundancy, the number of subcarriers should be kept within a reasonable range, and user distribution should be aligned with the subcarrier capacity.

SINR is the backbone of spectral efficiency, and both Inter-Carrier Interference (ICI) and Co-Channel Interference (CCI) directly affect it. As observed in performance evaluations conducted over the past ten years—and as examined within this thesis—ICI and CCI have an inversely proportional impact on spectral efficiency. Therefore, interference management is a critical aspect of maximizing spectral efficiency in OFDMA systems.

To ensure system consistency and realism, the modulation scheme is naturally implemented as OFDM when this multiple access method is used in the satellite constellation. Similar to the NOMA method, the SINR calculations and other simulation parameters stored in the system memory are kept constant under equal environmental conditions for the spectral efficiency simulations. In other words, the spectral efficiency corresponding to the average SINR is calculated.

Under the simulation conditions corresponding to Figure 5.6 (including the ICI and CCI coefficients and the number of subcarriers), the spectral efficiency values of the LEO satellite constellation employing the OFDMA multiple access method are illustrated in the heatmap below, as a function of the number of users within the coverage area and the number of satellites in the shell.

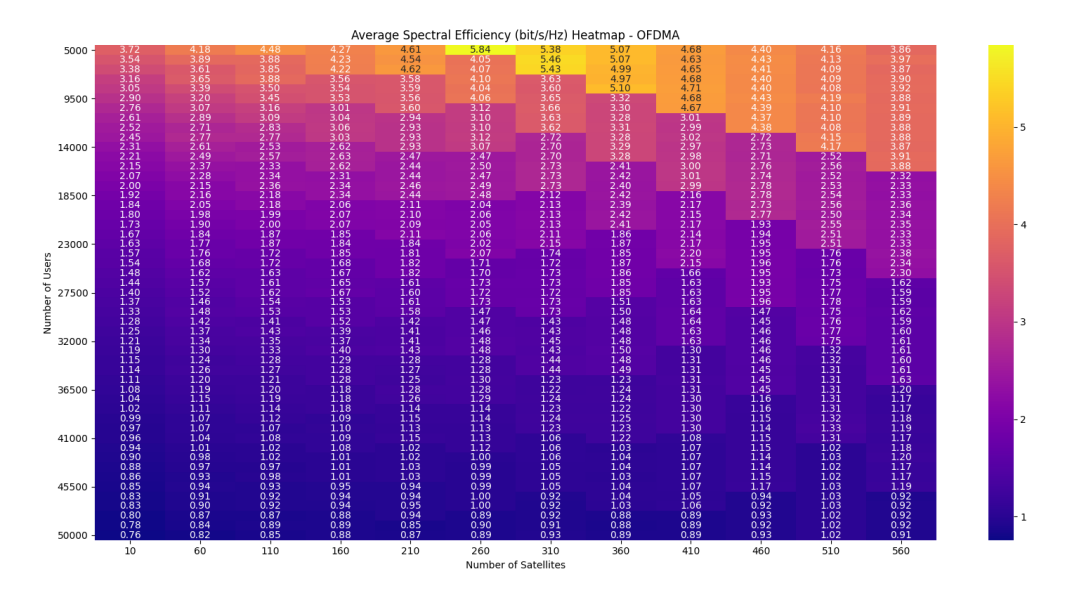


Figure 5.8: Spectral Efficiency Heatmap for OFDMA System

Figure 5.8. shows the average downlink spectral efficiency of OFDMA as a function of constellation size in case of  $N_{sc}=256$ . A wide optimum shows up at light load, maxing at approximately 5,8 bit/s/Hz around 260 satellites and 5,000 users; in the same load region values are above 5,0 bit/s/Hz for approximately 260–310 satellites. With increasing user numbers efficiency decreases monotonically because the fixed bandwidth of each satellite must now be shared by more and more users: for approximately 14,000–23,000 users typical values are in the 1,6–2,7 bit/s/Hz range, and for heavy load (< 41,000 users) the map converges near the region of 0,9–1,3 bit/s/Hz for the majority of constellation sizes. Densification of the shell benefits up to a moderate scale by boosting spatial reuse and link budgets, after which the benefits diminish and for very high constellations even start to move backwards. The outcomes match the set-up at the Ka-band frequency of 28 GHz by 100 MHz overall bandwidth in the presence of Rayleigh fading and by orthogonal allocation of sub-carriers for each.

According to the obtained results, it is observed that NOMA provides a wider spectral range and higher spectral efficiency than OFDMA in the satellite constellation simulation. This is an expected outcome since OFDMA is an orthogonal multiple access method, meaning the spectrum is divided among users, which indirectly reduces the system's spectral efficiency. Nevertheless, both multiple access techniques have their own trade-offs. A common trend becomes evident when analyzing the heatmap outputs of both methods: maximum spectral efficiency is observed when the average number of satellites that users communicate with during a given timestamp is around 2. When this ratio exceeds 3, spectral efficiency starts to decline. On the other hand, having only 1 user terminal per satellite is not a realistic scenario. In conclusion, the spectral efficiency outputs obtained from the simulation are realistic and within acceptable limits. A summary of the derived insights is presented in Table 5.1 below.

Table 5.1: Spectral Efficiency Comparison of NOMA and OFDMA

Criteria	NOMA	OFDMA
Maximum SE	7,46  bit/s/Hz	5,84  bit/s/Hz
Optimal configuration	$\approx 5,000$ users, $\approx 260$ satellites	$\approx 5,000$ users, $\approx 260$ satellites
SE degradation with user increase	Gradual and slower	Rapid and steep
Interference impact	Mitigated by SIC; residual remains	CCI and ICI have strong impact
Suitability for IoT	More suitable at light traffic	ICI issues present
SE optimisation parameters	SIC quality, power allocation	Subcarrier count, CCI/ICI mitigation

As in the SINR simulations, the spectral efficiency evaluations are carried out for the downlink Ka-band scenario ( $f_c \approx 28$  GHz) with a total bandwidth of 100 MHz. The simulations vary both the number of satellites (M) and the number of users (N) within a European coverage area, using a Walker-Delta shell at a fixed reference epoch. Satellites and user terminals are assumed to employ ideal parabolic antennas ( $\approx 50$  dBi gain, 1 m diameter) with a spot-beam architecture, while user-satellite links are modelled as independent Rayleigh-faded channels. Both inter-satellite and intra-satellite interference are included in the analysis, whereas inter-symbol interference (ISI) and atmospheric attenuation effects are disregarded.

## 5.3.6 System Capacity and Data Rates

In this section, we address the performance evaluations and system optimization required for the designed LEO satellite constellation to deliver high data rates and high capacity in the Ka band. In satellite communications, one of the most critical metrics is the system's total capacity. In LEO constellations, capacity is of course explained by the Shannon principle and is directly related to the sum-rate discussed theoretically in Chapters 3 and 4. In the simulation, the realized sum-rate is aggregated over users to obtain the total; that is, the total system capacity is computed for all satellites provided in varying numbers and for the varying number of users within their coverage areas. The same approach is followed when evaluating both multiple access methods.

At this stage of the simulation, the expected outcome is an increase in downlink capacity as the number of satellites grows. By performing interference management and tuning constellation parameters, we aim to achieve higher capacity and data-rate levels. In LEO satellite communications, the service time of a single satellite to users within its coverage area is short. Therefore, when considering constellations capable of providing continuous, high-speed service—as in this study—system optimization becomes crucial. In the literature, it is possible to find studies that analyze system capacity and compare mega-constellations [27]. Under identical conditions in the LEO constellation, the choice between NOMA and OFDMA affects two system metrics in distinct ways.

• System Capacity: The theoretical sum rate is determined by the multiple-access rate region. Considering the spectral efficiency analysis outputs, it could be expected that With ideal successive interference cancellation (SIC), NOMA can match or surpass OFDMA, especially when users with markedly different channel gains are paired. However, the advantage diminishes as the number of users increases or

their SINRs converge, and it can disappear under practical impairments such as residual SIC interference or suboptimal decoding order.

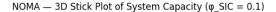
• Data Rates: In OFDMA, each user's rate is governed by the bandwidth and SINR on its orthogonal time-frequency resources. In NOMA, users share the same band, and rates are dictated by the power split and SIC decoding order—typically boosting the weaker user while requiring the stronger user to cede part of its rate, trading off fairness against sum-rate.

#### 5.3.7 System Performance Analysis of NOMA Downlink

The performance of the NOMA system is evaluated by user per satellite UPS value while the satellite number in the constellation is fixed as 260 since this is found as the optimum value for a constellation shell, which gives the highest average SINR for the users in the coverage area. For each combination of UPS and  $n_{\rm sats}$  (the number of satellites), the simulation models a single satellite's NOMA cluster of size UPS.

Within each cluster, a SIC-compatible Gain Ratio Power Allocation is applied, with small-scale fading and individual link distances generated for each user. An inter-satellite interference component is included, scaling proportionally with  $n_{\rm sats}$ . From the resulting user SINRs, the per-satellite capacity is computed as in Equation 3.9 and then it is aggregated for the chosen satellite count.

For a given UPS the same channel and interference realizations are reused across all values of  $\phi_{SIC}$ , ensuring that observed differences between curves are attributable solely to variations in the SIC residue. Obtained results for system capacity as line graph can be seen in the Figure 5.9.



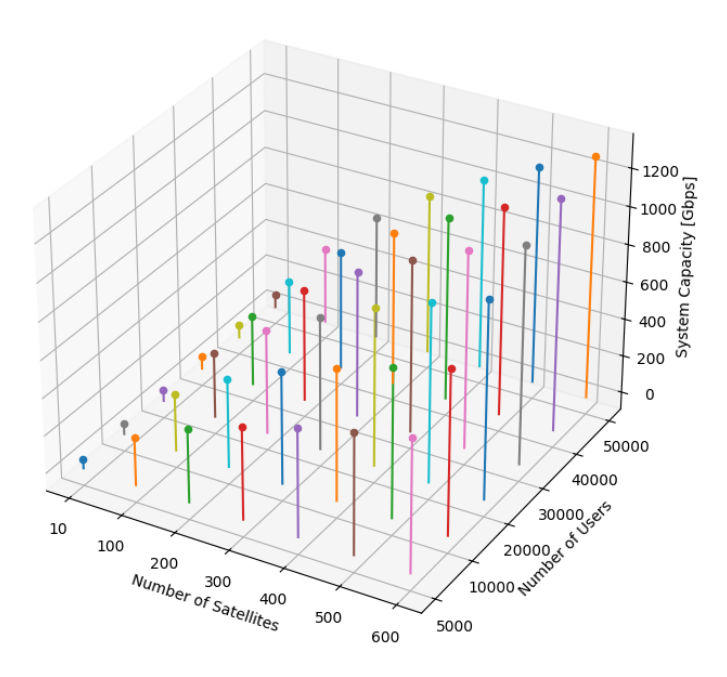


Figure 5.9: NOMA — System Capacity in Gbps

The figure reveals system capacity monotonically rising with the number of satellites and the number of users. On the sparse side capacity is around 0,1 Tbps. It passes 0,5 Tbps approximately at 260 satellites and around 20,000 users, and top 1 Tbps once the constellation achieves around 400-500 satellites and at least 30,000 users. The maximum attain the most dense sampled setting ( $\approx 560$  satellites and 50,000 users), in which the capacity reaches around 1,3–1,35 Tbps. With a given user load (e.g., around 30,000 users), the increase in satellites from 100 satellites to 560 satellites results in a three-to four-time increase in gain (from around 300 Gbps to around 1.1 Tbps), while a given constellation size (e.g., 400 satellites) and an increase in the number of users from 5,000 to 50,000 increase the capacity from around 350 Gbps to around 1,2 Tbps. In general, with low SIC residue, NOMA exhibits pronounced multiplexing gains through constellation densification and user aggregation within the evaluated LEO scenario.

To obtain the average data rate per user in the service area, simulation is compiled to allocate first the satellite's total transmit power among its users in a descending pattern, consistent with the principles of successive interference cancellation (SIC) decoding. The model incorporates two types of interference: (i) residual intra-cluster interference stemming from imperfect SIC, which is scaled by a chosen  $\phi_{SIC}$  parameter, and (ii) a statistical surrogate for inter-satellite interference based on sidelobe coupling. Three separate curves are generated by repeating the procedure for SIC residue factors.

$$\phi_{\text{SIC}} \in \{0.1, 0.5, 0.9\}. \tag{5.1}$$

Utilizing these parameters, the signal-to-interference-plus-noise ratio (SINR) for each

user is computed. The user's achievable data rate is then determined by converting the SINR using the satellite's bandwidth and a Shannon-type mapping. The per-satellite throughput is obtained by summing these individual user data rates. First, the satellite count in the constellation is chosen as 260, and in the 2nd scenario, the satellite count is decreased to 130, the half of the first value, to observe the constellation parameters' effect on the data rates.

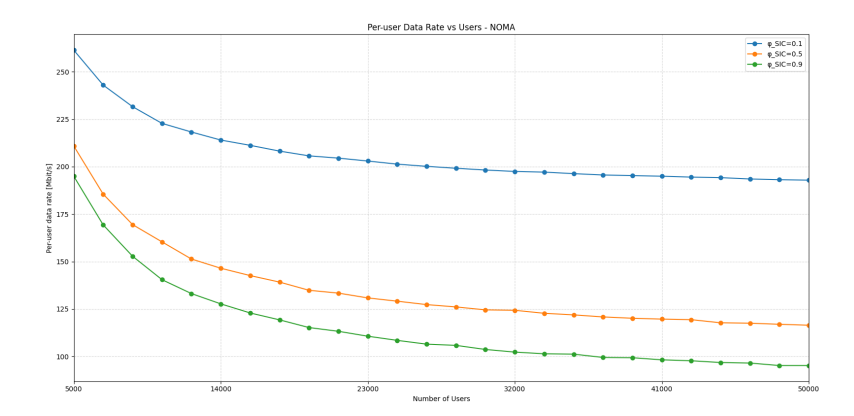


Figure 5.10: NOMA-Average Per-user Data Rate vs Users  $(n_{sats} = 260)$ 

Fig. 5.10. indicates the NOMA downlink average per-user data rate dependence for the fixed 260-satellite constellation and different SIC residue parameter values of  $\phi_{\rm SIC}$ . The results confirm a steep monotonic decline in the rate for rising user burden: at low burden around 5,000 users, the optimum value is about 261Mbit/s for the parameter value of  $\phi_{\rm SIC}=0.1$ , while in comparison 210Mbit/s and 195Mbit/s are obtained for the parameter values of  $\phi_{\rm SIC}=0.5$  and  $\phi_{\rm SIC}=0.9$ , respectively. As the burden draws closer to 50,000 users, rates converge in the 190–200Mbit/s range and the desirable SIC performance is consistently paired by a larger value. The discrepancy in the lines is the greatest at low burden and the high-efficiency intra-cluster interference reduction by a few clusters benefits the performance largely and gradually diminishes along the rising user increase continuation, due to the fact that the intra-cluster interference tends to dominate. In general terms, the figure shows the double task in assuring high user rates by constellation density and SIC quality and unveils the reality that desirable interference suppression mainly favors light traffic scenarios while at the same time offering good performance at high constellation density.

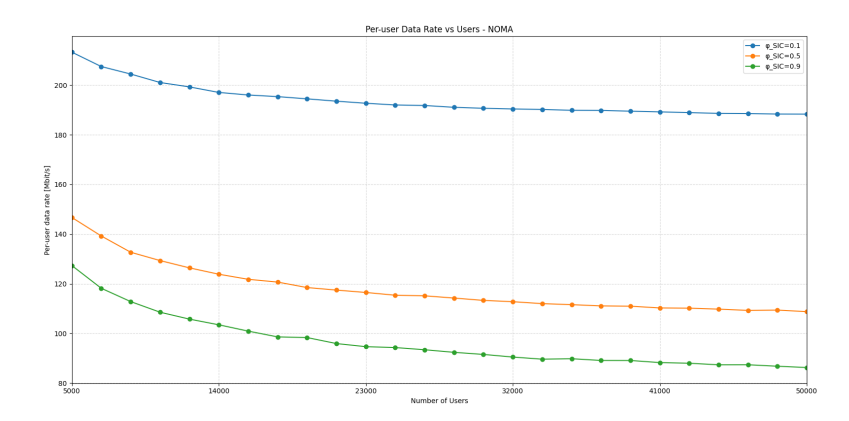


Figure 5.11: NOMA-Average Per-user Data Rate vs Users  $(n_{sats} = 130)$ 

Figure 5.11. depicts average per-user data rate for NOMA with  $n_{\rm sats}=130$  as a function of growing user population for three SIC residue levels  $\varphi_{\rm SIC} \in [0.1,0.5,0.9]$ . The lines fall gradually as the load increases because power is distributed across more and more users and residual intra-cluster interference grows. With near-ideal SIC the rate starts around 213, Mbit/s and stays above 188Mbit/s; with moderate SIC it falls from about 146Mbit/s down to 109Mbit/s; with poor SIC it falls from about 127Mbit/s down to  $\sim 86$ Mbit/s. The fixed difference between the three traces highlights the benefit of better interference suppression. Compared with the  $n_{\rm sats}=260$  case, all values are lower since a higher user-to-satellite ratio leaves less power per user and increases residual interference under the same Ka-band and channel assumptions.

Table 5.2: Maximum and Minimum Per-User Data Rates

	$n_{sats}$	= 130	$n_{sats} = 260$	
$\phi_{SIC}$	Max Rate (Mbit/s)	Min Rate (Mbit/s)	Max Rate (Mbit/s)	Min Rate (Mbit/s)
0.1	220,3	189,3	261,1	192,5
0.5	147,5	109,8	211,7	117,2
0.9	128,4	87,5	195,3	96,6

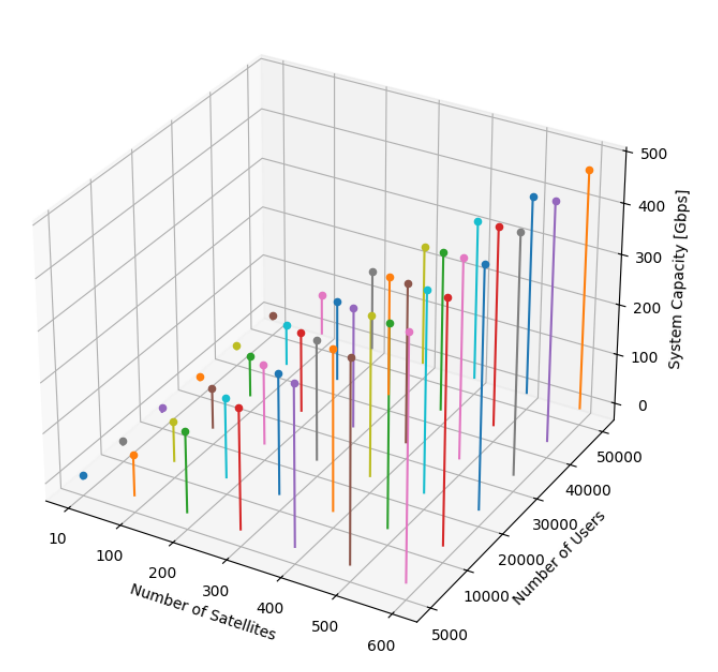
#### 5.3.8 System Performance Analysis of OFDMA Downlink

The simulation utilizing the OFDMA method was regenerated, and the system capacity and average per-user data rate were calculated based on the methodology described in Chapter 4.2.5 of this study. A significant difference from the NOMA method in this implementation is the consideration of frequency division provided by orthogonal subcarriers. System capacity increases with the number of subcarriers, but due to ICI and CCI effects, an unlimited capacity is not possible. Thus, SINR and data rate will be optimized and remain at a certain level.

In the simulation phase, the per-satellite capacity was first determined, and the formula was generalized to obtain the system capacity.  $\Delta f_n$  is a critical factor when calculating the per-user data rate (Equation 4.14). At this point, each subcarrier is assumed

to have the same average SINR values. The system bandwidth was set to 100 MHz for the intended service in the Ka-band, a suitable value for the frequency band and target applications.

The simulation results were shared for fairness, similar to the NOMA model. A 3D stick plot will be used to calculate the total system capacity concerning the number of users and satellites, followed by line graphs to show the per-user data rate. The effects of the number of satellites and the number of subcarriers used in modulation on the data rate will be examined. An initial value of 260 satellites, which provides the optimum system SINR as proven in Chapter 5.3.2., was selected. This value was then halved to 130 to analyze the effect of the number of satellites, a constellation parameter, on the system. Total system capacity of the LEO constellation using OFDMA multiple access method can be seen by changing number of satellites and users in coverage area in Figure 5.12



OFDMA — 3D Stick Plot of System Capacity, (Nsc=256)

Figure 5.12: OFDMA — System Capacity in Gbps

Figure 5.12. claims that the obtained maximum system capacity is 473,53 Gbps, with  $N_{sc}=256$  per satellite to achieve a higher capacity. A reasonable and satisfactory result for the targeted IoT and high-speed internet applications in the Ka-band. Maximizing capacity relies on a fair and extensive allocation of bandwidth. Another critical factor is channel modeling. Both systems were tested with a Rayleigh fading channel model. Different channel models, (e.g. Frequency-Selective Fading), could yield even higher capacity results for OFDM [28] and consequently for OFDMA.

To evaluate system performance, the next step in the calculation is to determine the average data rate per user. To achieve this, the SINR and sum rate formulas for OFDMA, as defined in the simulation, were first converted into a function (Equation 4.3). Subsequently, the number of satellites was initially fixed at 260, which provides the system's highest SINR value. With this configuration, the LEO constellation began serving a fluctuating number of user terminals, ranging from 5,000 to 50,000, with 260 satellites.

In the second scenario, the number of satellites was reduced to 130 to investigate the effects of decreased density within the shell and reduce inter-satellite interference. Three scenarios were then examined, where the number of orthogonal subcarriers per satellite was varied among 64, 128, and 256. While an increase in the number of subcarriers does not affect the data rate directly, however it changes the  $\Delta f_n$  and it causes greater Doppler effect on the LEO satellite.

The primary objective is to observe the maximum data rate that two different constellation parameters: The number of satellites and the number of subcarriers per satellite can provide to user terminals within the service area. This is a critical output for achieving sensitive and high-speed communication in the frequency band used. Obtained results are shown in the Figure 5.13 and Figure 5.14

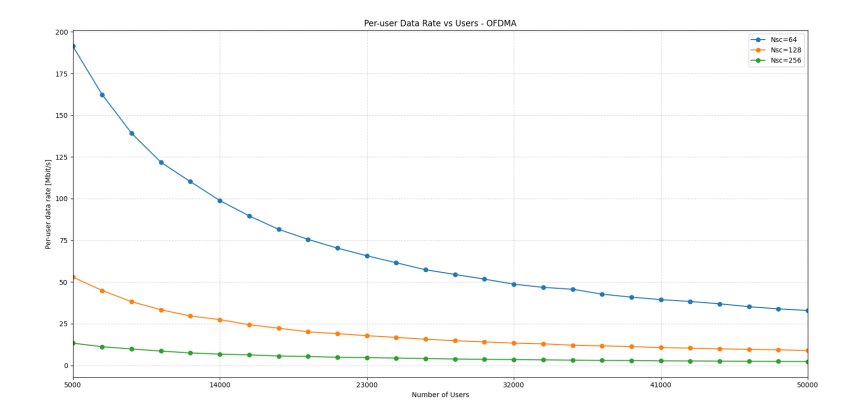


Figure 5.13: OFDMA-Average Per-user Data Rate vs Users  $(n_{sats} = 260)$ 

Figure 5.13 depicts per-user average data rate for an OFDMA downlink featuring 260 satellites and three subcarrier allocations ( $N_{sc}=64,128,256$ ). With greater numbers of users, rates decrease due to shared subcarriers and interference. With  $N_{sc}=64$ , rates are in excess of 190 Mbit/s at 5,000 users and are in the range 33–35 Mbit/s at 50,000. For  $N_{sc}=128$ , from 53 to 9–10 Mbit/s; and for  $N_{sc}=256$ , from 13–14 to 2–3 Mbit/s. Increasing numbers of subcarriers increase Doppler sensitivity and inter-carrier interference, so gains are reduced. For this reason, moderate subcarrier numbers are optimal in terms of spectral efficiency-robust.

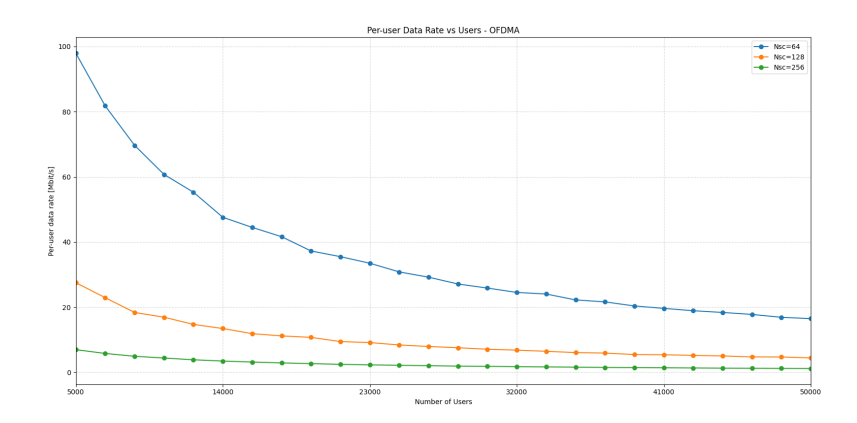


Figure 5.14: OFDMA-Average Per-user Data Rate vs Users  $(n_{sats} = 130)$ 

Figure 5.14. shows the average per-user data rate in the OFDMA downlink when the constellation size is reduced to  $n_{sats}=130$ , with three different subcarrier settings,  $N_{sc}\in[64,128,256]$ . The curves display the same downward trend with increasing user numbers as in the 260-satellite scenario, but the overall values are lower since each satellite serves more users and residual interference becomes stronger. With  $N_{sc}=64$ , the rate begins at about 98 Mbit/s for 5,000 users and steadily falls to around 16–17 Mbit/s at 50,000 users. For  $N_{sc}=128$ , it drops from roughly 27–28 Mbit/s to 4–5 Mbit/s, while  $N_{sc}=256$  offers only 6–7 Mbit/s under light load and falls below 2 Mbit/s at heavy load. These results highlight how cutting the constellation size in half sharply reduces per-user performance, as the increased user-to-satellite ratio outweighs any advantage from finer spectral partitioning. The figure illustrates that, under realistic Ka-band LEO conditions, both constellation density and the choice of subcarrier number are critical in maintaining satisfactory data rates.

An examination of the results indicates that an exponential increase in the number of subcarriers exacerbates Doppler-related effects and co-channel interference (CCI), thereby reducing the achievable per-user data rates. It should be noted that a LEO satellite's typical coverage time is approximately 8–10 minutes [29]. Consequently, continuous handovers occur among satellites within the same shell of the constellation, whereby user terminals are frequently reassigned between satellites. When this effect is considered, the attained data-rate values are consistent with the target user base and the intended service objectives. As expected, reducing the number of satellites leads to a decline in aggregate data rate.

Under the configuration  $N_{\rm sc}=64$ , a reasonable and acceptable data-rate performance is observed. Therefore, for a coverage area with a variable user population between 5,000 and 50,000 and assuming a per-satellite system bandwidth of 100 MHz, choosing 64 subcarriers constitutes an appropriate optimization decision.

Table 5.3: Maximum and Minimum Per-User Data Rates

	$n_{sats}$ :	= 130	$n_{sats} = 260$	
$N_{sc}$	Max Rate (Mbit/s)	Min Rate (Mbit/s)	Max Rate (Mbit/s)	Min Rate (Mbit/s)
64	98,1	16,5	191,1	33,4
128	27,5	$4,\!4$	53	9,3
256	7	1,3	14	2

An increase in the number of subcarriers results in a longer OFDM symbol duration, which in turn amplifies the system's vulnerability to pronounced Doppler shifts arising from the high orbital velocities of LEO satellites. Such Doppler impairments compromise subcarrier orthogonality, thereby inducing considerable inter-carrier interference (ICI). Consequently, in the absence of robust and real-time Doppler compensation in conjunction with advanced adaptive resource allocation strategies, a reduction in the average per-user data rate with increasing subcarrier count in LEO Ka-band OFDMA systems is both a realistic and frequently anticipated outcome. The relationship between subcarrier count and achievable data rate is inherently nonlinear, governed by intricate trade-offs among inter-symbol interference (ISI) suppression, susceptibility to ICI, and the operational efficacy of adaptive resource management under dynamic channel conditions.

### Chapter 6

## Conclusion and Future Work

In scope of this thesis, a LEO satellite communication simulation was implemented in the Python 3.10 software environment. This simulation has a variable number of satellites and user terminals served in a coverage area within a dedicated timestamp. The objective throughout the study was to use the created simulator to conduct performance calculations for NOMA and OFDMA multiple access methods, which are rapidly evolving and used in the  $5\mathrm{G}/6\mathrm{G}$  communication field, and to achieve system optimisation. In this context, the computational outputs examined were Signal-to-Interference-plus-Noise Ratio, Spectral Efficiency, System Capacity, and Data Rates.

This study shows that NOMA is a highly promising technique for maximizing the use of scarce satellite spectrum in LEO constellations. By allowing multiple users to share the same frequency and time resources, NOMA significantly boosts system capacity and user data rates. A key finding is that NOMA's performance, particularly in terms of SINR, remains strong even with deliberate inter-user interference. This is because users with stronger signals can cancel out the interference from weaker signals using a process called SIC, while weaker users receive enough power to decode their own data successfully. This effective management of interference leads to a better overall SINR distribution compared to OFDMA. However, the benefits of NOMA decrease if SIC residual factor cannot be designed optimally.

Although NOMA method offers high spectral efficiency and faster data rates, the research also highlights specific situations where OFDMA is preferable. In environments with minimal Doppler shift—like slow-moving users or near-equatorial LEO orbits—OFDMA performs well because its main weakness, sensitivity to rapid frequency changes, is not a factor. In these stable conditions, OFDMA can achieve throughput similar to NOMA without the added complexity of SIC. OFDMA is also a better option when a network needs to guarantee high fairness or a uniform quality of service to all users. Since OFDMA dedicates separate resources to each user, it naturally avoids inter-user interference and makes it easier to provide consistent performance across the board [30]. In contrast, ensuring fairness with NOMA can require more complex strategies.

Also it should be noted that, particularly for the NOMA simulations, the physical layer was not fully implemented into simulator and the behaviour of the actual waveforms was not explicitly modelled. Accordingly, SIC was represented in simplified approach by a

scalar efficiency factor and a residual-interference term. This modelling choice reflects the capabilities of the simulator and was adopted to keep the computational burden within reasonable limits.

When it comes to possible future studies, considering the rapidly growing satellite communication industry's increasing investment in mega constellations, the importance of multiple access methods is growing over time. This study was a satellite constellation research project providing communication in the Ka-band and offering IoT applications and high-speed internet services. It is certain that the multiple access methods examined will exhibit different performance levels across different frequency bands (e.g., Ku-band, K-band). A much broader study addressing all these aspects could be conducted. Essentially, no multiple access method can be flawlessly superior to another multiple access method without trade-offs or negative effects. The hybrid use of NOMA and OFDMA methods in a satellite constellation is technically feasible, and the results obtained may be more efficient than those achieved using only the NOMA method for multiple access. However, the impact of different antenna designs and gains on these multiple access methods can also be observed. In this study, a spot beam architecture was used; in future studies, different beam architectures could be implemented in satellite terminals.

These methods are crucial for building advanced LEO satellite networks. They will lead to higher data speeds and more efficient use of the radio spectrum, ensuring that a wide range of users and devices, from IoT sensors to broadband internet customers, can all connect fairly. By following these approaches, researchers and engineers can solve current problems and improve how multiple devices connect to LEO satellite networks. Ultimately, these steps pave the way for the next generation of space-based communications.

# **Bibliography**

- [1] A. Zanella, N. Bui, A. Castellani, L. Vangelista, and M. Zorzi, "Internet of things for smart cities," *IEEE Internet of Things Journal*, vol. 1, no. 1, pp. 22–32, Feb. 2014.
- [2] M. Mahbub and R. M. Shubair, "Contemporary advances in multi-access edge computing: A survey of fundamentals, architecture, technologies, deployment cases, security, challenges, and directions," *Journal of Network and Computer Applications*, vol. 219, p. 103726, 2023.
- [3] (2023) Satellite regulation: Leo, geo, wrs. Accessed 9 Sep 2025. [Online]. Available: https://www.itu.int/hub/2023/01/satellite-regulation-leo-geo-wrs/
- [4] Types of orbits. European Space Agency (ESA). Accessed 9 Sep 2025. [Online]. Available: https://www.esa.int/Enabling\_Support/Space\_Transportation/Types\_ of orbits
- [5] T. Pratt and J. E. Allnutt, Satellite Communications. Wiley-Blackwell, 2020.
- [6] D. Nieto Yll, "Doppler shift compensation strategies for leo satellite communication systems," B.S. thesis, Escola Tècnica d'Enginyeria de Telecomunicació de Barcelona, Universitat Politècnica de Catalunya, Barcelona, Spain, Jun. 2018.
- [7] H. Ben Salem, A. Tarable, A. Nordio, and B. Makki, "Uplink soft handover for leo constellations: how strong the inter-satellite link should be," arXiv preprint arXiv:2403.15131, Mar. 2024, accessed 9 Sep 2025. [Online]. Available: https://arxiv.org/abs/2403.15131
- [8] V. Agrawal and A. K. Maini, Satellite Technology: Principles and Applications, 3rd ed. Wiley, n.d., n.d.
- [9] Channel access method. Wikipedia. Accessed 9 Sep 2025. [Online]. Available: https://en.wikipedia.org/wiki/Channel\_access\_method
- [10] D. S. Ilcev, "Analyses of space division multiple access (sdma) schemes for global mobile satellite communications (gmsc)," Durban University of Technology, Durban, South Africa, Tech. Rep., n.d.
- [11] National institutes of health PMC article 8271421. Accessed 9 Sep 2025. [Online]. Available: https://pmc.ncbi.nlm.nih.gov/articles/PMC8271421/
- [12] A. T. Abusabah and H. Arslan, "Noma for multinumerology OFDM systems," Electrical Engineering Faculty Publications, University of South Florida, 2018, accessed 9 Sep 2025. [Online]. Available: https://digitalcommons.usf.edu/ege\_facpub/11
- [13] H. Mathur and T. Deepa, "A novel precoded digitized OFDM based NOMA system for future wireless communication," *Optik*, vol. 259, p. 168948, 2022.

- [14] Electronic Communications Committee (ECC), "The use of the frequency bands 27.5–30.0 ghz and 17.3–20.2 ghz by satellite networks," Electronic Communications Committee (ECC) within the European Conference of Postal and Telecommunications Administrations (CEPT), Tech. Rep. ECC Report 152, Sep. 2010, accessed: 9 Sep. 2025. [Online]. Available: https://docdb.cept.org/download/616
- [15] K. Chen-Hu, M. M. Céspedes, and A. G. Armada, "Ofdm-based multicarrier transmission," in Wiley 5G Ref, R. Tafazolli, C.-L. Wang, and P. Chatzimisios, Eds. Wiley, 2020. [Online]. Available: https://doi.org/10.1002/9781119471509. w5GRef001
- [16] O. Özdemir, R. Hamila, and N. Al-Dhahir, "Exact average OFDM subcarrier SINR analysis under joint transmit-receive i/q imbalance."
- [17] Q. Zhu, Z. Chen, and X. He, "Resource allocation for relay-based OFDMA power line communication system," *Electronics*, vol. 8, no. 2, p. 125, 2019.
- [18] P. Tan and N. C. Beaulieu, "Reduced ICI in OFDM systems using the better than raised-cosine pulse," n.d., IEEE COMMUNICATIONS LETTERS, VOL. 8, NO. 3, MARCH 2004.
- [19] B. Da and R. Zhang, "Cooperative interference control for spectrum sharing in OFDMA cellular systems," *IEEE Transactions on Signal Processing*, vol. 58, no. 8, pp. 4205–4218, Aug. 2010.
- [20] S. K. Thaherbasha, N. Durga Rao, and P. Balakrishna, "Evaluation of spectral efficiency of cellular OFDMA system compared with FDMA, TDMA, CDMA and WCDMA," *International Journal of Creative Research Thoughts (IJCRT)*, vol. 6, no. 1, pp. 1–6, Mar. 2018.
- [21] S. Martínez Zamacola, S. Martín Marco, and R. Martínez Rodríguez-Osorio, "Profiling the transmit power of LEO satellite constellations for broadband communication services considering terrestrial and aerial demand," Acta Astronautica, vol. 236, pp. 547–559, 2025.
- [22] X. Li, B. Shang, Q. Wu, and C. Ren, "Coverage and spectral efficiency of NOMA-enabled LEO satellite networks with ordering schemes."
- [23] K.-X. Li, X. Gao, and X.-G. Xia, "Channel estimation for LEO satellite massive MIMO OFDM communications," *IEEE Transactions on Wireless Communications*, vol. 21, no. 10, pp. 8900–8914, Oct. 2022.
- [24] S. B. Mosunmola, A. O. Agboola, A. Felix, and A. Mohammed, "The mathematical model of doppler frequency shift in leo at ku, k and ka frequency bands," *International Journal of Trend in Research and Development (IJTRD)*, vol. 4, no. 5, Oct. 2017, accessed 9 Sep 2025. [Online]. Available: http://www.ijtrd.com/papers/IJTRD12035.pdf
- [25] I. Leyva-Mayorga, V. Gala, F. Chiariotti, and P. Popovski, "Continent-wide efficient and fair downlink resource allocation in LEO satellite constellations," in *IEEE ICC* 2023, 2023, short citation; see detailed entry [31].
- [26] D. Rozenvasser and K. Shulakova, "Estimation of the starlink global satellite system capacity," *Proceedings of the International Conference on Applied Innovations in IT*, vol. 11, no. 1, pp. 55–59, Mar. 2023, köthen, Germany, 9 March 2023.

- [Online]. Available: https://opendata.uni-halle.de/bitstream/1981185920/103863/ $1/1_9\%20$ ICAIIT\_2023\_paper\_4290.pdf
- [27] I. del Portillo, B. G. Cameron, and E. F. Crawley, "A technical comparison of three low earth orbit satellite constellation systems to provide global broadband," *Acta Astronautica*, vol. 159, pp. 123–135, Jun. 2019, open Access version at DSpace@MIT. [Online]. Available: https://dspace.mit.edu/handle/1721.1/135044.2
- [28] Z. Shen, J. G. Andrews, and B. L. Evans, "Optimal power allocation in multiuser OFDM systems," in *Proceedings of the IEEE Global Telecommunications Conference* (GLOBECOM'03), vol. 1. San Francisco, CA, USA: IEEE, Dec. 2003, pp. 337–341. [Online]. Available: https://users.ece.utexas.edu/~bevans/papers/2003/multiuserOFDM/multiuserOFDMGlobecom2003Paper.pdf
- [29] E. Kang, Y. Park, J. Kim, and H. Choo, "Downlink analysis of a low-earth orbit satellite considering an airborne interference source moving on various trajectory," *Remote Sensing*, vol. 16, no. 2, p. 321, 2024. [Online]. Available: https://doi.org/10.3390/rs16020321
- [30] P. Xu and K. Cumanan, "Optimal power allocation scheme for non-orthogonal multiple access with  $\alpha$ -fairness," *IEEE Journal on Selected Areas in Communications*, vol. 35, no. 10, pp. 2357–2369, Oct. 2017, article no. 7986959. [Online]. Available: https://doi.org/10.1109/JSAC.2017.2729780
- [31] I. Leyva-Mayorga, V. Gala, F. Chiariotti, and P. Popovski, "Continent-wide efficient and fair downlink resource allocation in LEO satellite constellations," in *ICC 2023 IEEE International Conference on Communications: Sustainable Communications for Renaissance*, 2023, pp. 6689–6694.